JEM Journal of Experimental Medicine

ARTICLE

TGF-β promotes stem-like T cells via enforcing their lymphoid tissue retention

Chaoyu Ma[1], Liwen Wang[1,4], Wei Liao[1,2], Yong Liu[3,6,7,8], Shruti Mishra[1], Guo Li[1,3,6,7], Xin Zhang[3,6,7,8], Yuanzheng Qiu[3,6,7,8], Qianjin Lu[2,5], and Nu Zhang[1]

Stem-like CD8⁺ T cells sustain the antigen-specific CD8⁺ T cell response during chronic antigen exposure. However, the signals that control the maintenance and differentiation of these cells are largely unknown. Here, we demonstrated that TGF-β was essential for the optimal maintenance of these cells and inhibited their differentiation into migratory effectors during chronic viral infection. Mechanistically, stem-like CD8⁺ T cells carried a unique expression pattern of α4 integrins (i.e., α4β1^{hi} and α4β7^{lo}) controlled by TGF-β. In the absence of TGF-β signaling, greatly enhanced expression of migration-related markers, including altered expression of α4 integrins, led to enhanced egress of stem-like CD8⁺ T cells into circulation accompanied by further differentiation into transitional states. Blocking α4 integrin significantly promoted their lymphoid tissue retention and therefore partially rescued the defective maintenance of Tcf-1⁺ subset in the absence of TGF-β signaling. Thus, TGF-β promotes the maintenance and inhibits the further differentiation of stem-like T cells at least partially via enforcing their lymphoid tissue residency.

Introduction

During chronic antigen exposure, effector T cells enter an exhausted state (Hashimoto et al., 2018; McLane et al., 2019). A subset of less exhausted CD8⁺ T cells carry unique markers including chemokine receptor CXCR5 and transcription factor Tcf-1 and behave like stem cells or progenitors to sustain T cell response (He et al., 2016; Im et al., 2016; Leong et al., 2016; Utzschneider et al., 2016; Wu et al., 2016). Tcf-1⁺ stem-like CD8⁺ T cells are largely confined to the secondary lymphoid tissues (He et al., 2016; Im et al., 2016) and do not enter the circulation, similar to tissue-resident cells (Im et al., 2020). This unique location is conserved between mouse and human (Miron et al., 2018). Even though stem-like CD8⁺ T cells have been identified among tumor-infiltrating T cells (Brummelman et al., 2018; Kurtulus et al., 2019; Miller et al., 2019; Sade-Feldman et al., 2018; Siddiqui et al., 2019), which by definition is outside a secondary lymphoid tissue, a T cell zone-like local environment exists inside solid tumors to host these stem-like CD8⁺ T cells (Jansen et al., 2019). Thus, the retention inside secondary lymphoid organs or similar microenvironment may be essential for stem-like CD8⁺ T cells. Leaving such environment may be associated with further differentiation accompanied by the loss of stemness. However, the signals or mechanisms controlling the migration or retention of stem-like CD8⁺ T cells are largely unknown.

TGF-β is generally considered a negative regulator of immune responses during chronic infection or anti-tumor immunity (Giordano et al., 2015; Park et al., 2016; Tinoco et al., 2009). TGF-β inhibitor has been successfully combined with checkpoint blockade therapy to improve tumor control (Mariathasan et al., 2018; Tauriello et al., 2018). Intriguingly, TGF-β has been identified as a potent inducer of CXCR5 expression on effector CD8⁺ T cells during in vitro culture (Mylvaganam et al., 2017), suggesting a possible role of TGF-β in stem-like CD8⁺ T cells. Recently, it has been demonstrated that TGF-β promotes Tcf-1⁺ stem-like T cells via controlling mTOR activity and preserves

[1]Department of Microbiology, Immunology and Molecular Genetics, Long School of Medicine, University of Texas Health Science Center at San Antonio, San Antonio, TX; [2]Department of Dermatology, Hunan Key Laboratory of Medical Epigenomics, The Second Xiangya Hospital, Central South University, Changsha, Hunan, China; [3]Department of Otolaryngology Head and Neck Surgery, Xiangya Hospital, Central South University, Changsha, Hunan, China; [4]Department of Hematology, The Third Xiangya Hospital, Central South University, Changsha, Hunan, China; [5]Hospital for Skin Diseases (Institute of Dermatology), Chinese Academy of Medical Sciences and Peking Union Medical College, Nanjing, China; [6]Otolaryngology Major Disease Research Key Laboratory of Hunan Province, Xiangya Hospital, Central South University, Changsha, Hunan, China; [7]Clinical Research Center for Laryngopharyngeal and Voice Disorders in Hunan Province, Xiangya Hospital, Central South University, Changsha, Hunan, China; [8]National Clinical Research Center for Geriatric Disorders, Xiangya Hospital, Central South University, Changsha, Hunan, China.

Correspondence to Nu Zhang: zhangn3@uthscsa.edu

W. Liao's present address is Department of Dermatology, Hunan Children's Hospital, Changsha, Hunan, China. S. Mishra's present address is Department of Cancer Immunology and Virology, Dana-Farber Cancer Institute, Harvard Medical School, Boston, MA.

mitochondrial capacity during chronic viral infection (Gabriel et al., 2021). In addition to metabolic regulation, whether TGF-β controls the migration and localization of stem-like T cells remains unknown. Here, using TGF-β receptor–deficient CD8⁺ T cells, we show that TGF-β promotes stem-like CD8⁺ T cells, especially during the late stages of chronic viral infection. The defect in TGF-β receptor–deficient cells is partially due to dramatically altered expression of α4 integrins, which leads to enhanced egress of stem-like CD8⁺ T cells into circulation accompanied by subsequent differentiation into transitional effector T cells.

Results

TGF-β promotes stem-like CD8⁺ T cells

To determine the role of TGF-β in antigen-specific stem-like CD8⁺ T cells, we employed LCMV (lymphocytic choriomeningitis virus) Clone 13 infection model and TGF-β receptor II conditional knockout (*Tgfbr2*$^{f/f}$ distal *Lck*-cre, hereafter referred to as *Tgfbr2*$^{-/-}$) P14 TCR transgenic mice (Ma et al., 2017) that carried CD8⁺ T cells specific for LCMV epitope H-2D^{b}-GP$_{33-41}$. As illustrated in Fig. 1 A, naive P14 T cells carrying distinct congenic markers were isolated from WT control and *Tgfbr2*$^{-/-}$ mice, mixed at a 1:1 ratio, and adoptively co-transferred into unmanipulated sex-matched C57BL/6 (B6) recipient mice followed by LCMV Cl13 infection. In this system, WT control P14 T cells and *Tgfbr2*$^{-/-}$ ones are compared side-by-side in the same WT environment. Percentage-wise, early after infection, there were no significant changes in the induction of CXCR5 (Fig. S1, A and B) or Tcf-1 (Fig. 1, B and C) in donor P14 T cells lacking TGF-β receptor. However, as the infection progressed, a dramatic reduction of CXCR5⁺ and Tcf-1⁺ percentage was observed in *Tgfbr2*$^{-/-}$ cells (Fig. 1, B and C; and Fig. S1, A and B). As we have reported before, there was a decrease in the expansion of *Tgfbr2*$^{-/-}$ CD8⁺ T cells during both acute and chronic infections (Ma and Zhang, 2015; Zhang and Bevan, 2013). Thus, when focusing on the total number of Tcf-1⁺ vs. Tcf-1⁻ subsets, *Tgfbr2*$^{-/-}$ cells exhibited a two- to threefold reduction for both subsets at early stages. In contrast, at day 22 after infection, Tcf-1⁺ subset was specifically reduced while Tcf-1⁻ one was apparently normal in the absence of TGF-β receptor (Fig. 1 D). CD39 has been identified as an exhaustion marker while CD73 has been associated with CXCR5⁺ subset (Gupta et al., 2015; Im et al., 2016). CD39^{lo}CD73^{hi} cells were almost exclusively limited to Tcf-1⁺ subset (Fig. S1 C). In the absence of TGF-β receptor, CD39^{lo}CD73^{hi} cells were dramatically reduced (Fig. S1 D). Interestingly, the defects of CD73 induction occurred from the early stages of the infection, presumably due to the fact that CD73 was a direct target of TGF-β signaling in T cells (Chen et al., 2019; Takimoto et al., 2010). In addition, several other surface markers associated with CXCR5⁺Tcf-1⁺ subset (e.g., Ly6C, CXCR3, and CD62L) were similarly defective in *Tgfbr2*$^{-/-}$ cells at later stages of the infection (Fig. S1, E and F). Because stem-like CD8⁺ T cells are associated with poly-functionality, consistent with defective maintenance of stem-like subset, IL-2 production was greatly reduced at late, but not early stage of Cl13 infection in the absence of TGF-β signaling (Fig. 1 E).

TGF-β is critical for Tcf-1⁺ stem-like subset. We wondered whether Tcf-1⁺ and Tcf-1⁻ cells received differential TGF-β signaling in vivo. We did detect a slight trend of higher pSmad2/3 signal in Tcf-1⁺ cells although it did not reach statistical significance (Fig. S1 G). In addition, when WT and *Tgfbr2*$^{-/-}$ P14 T cells were separately transferred into different B6 recipients, we did not observe a dramatic difference in viral clearance or tissue pathology (Fig. S2, C and E). Transient depletion of CD4⁺ T cells prolonged the viremia. Side-by-side comparison demonstrated that the maintenance of stem-like CD8⁺ T cells required TGF-β both in the presence and the absence of CD4 help (Fig. S2, A and B). In the following experiments, we chose to use LCMV Cl13 infection without CD4 depletion. Together, TGF-β promotes stem-like CD8⁺ T cells during chronic viral infection.

TGF-β controls α4 integrins

We have previously discovered that TGF-β inhibits integrin α4β7 expression on effector CD8⁺ T cells during chronic LCMV infection (Zhang and Bevan, 2013). Thus, using the same experimental system, we have identified two seemingly distinct defects in *Tgfbr2*$^{-/-}$ cells, which are (1) enhanced α4β7 integrin expression and (2) defective stem-like CD8⁺ T cells. We wondered whether these two phenotypes were related or independent. We first examined the expression of α4 integrins on Tcf-1⁺ vs. Tcf-1⁻ CD8⁺ T cell subsets. Interestingly, we found that on WT cells, the expression of integrin α4β7 was almost exclusively restricted to Tcf-1⁻ subset (Fig. 1 F). However, in the absence of TGF-β receptor, the expression of α4β7 integrin was significantly increased, especially on Tcf-1⁺ subset (Fig. 1, F and H). There are two α4-containing integrin heterodimers on T cells, namely, integrin α4β1 and α4β7. Consistent with the restricted expression of α4β7 on WT Tcf-1⁻ cells, β1 integrin was dominant on stem-like Tcf-1⁺ subset while β1 and β7 co-expressed on the majority of Tcf-1⁻ subset (Fig. 1 G). On *Tgfbr2*$^{-/-}$ cells, the expression of β7 integrin was substantially increased on Tcf-1⁺ cells accompanied by reduced expression of β1 integrin (Fig. 1, G–I). β1 and β7 co-expressing cells were significantly enhanced in *Tgfbr2*$^{-/-}$ cells, especially in Tcf-1⁺ stem-like subset (Fig. 1 G right panel). To be noted, altered expression of α4-containing integrins on *Tgfbr2*$^{-/-}$ cells occurred as early as day 7–10 after infection (Fig. 1, F–I). To further validate these findings, we measured integrin ligand binding. As shown in Fig. S3, compared with WT counterparts, *Tgfbr2*$^{-/-}$ Tcf-1⁺ cells exhibited significantly higher α4β7 ligand (i.e., mucosal vascular addressin cell adhesion molecule-1 [MAdCAM-1]) binding and slightly reduced α4β1 ligand (i.e., vascular cell adhesion molecule-1 [VCAM-1]) binding. Importantly, the altered integrin ligand binding could be detected as early as day 10 (Fig. S3). Thus, we have shown that integrin β1 and β7 exhibits distinct expression pattern on Tcf-1⁺ vs. Tcf-1⁻ CD8⁺ T cells. The vast majority of WT Tcf-1⁺ cells only express β1 integrin while a significant portion of *Tgfbr2*$^{-/-}$ Tcf-1⁺ ones carry slightly reduced β1 and dramatically increased β7 integrins, resembling WT Tcf-1⁻ effectors.

TGF-β is essential for lymphoid tissue retention of Tcf-1⁺ cells

Because stem-like CD8⁺ T cells are commonly restricted to lymphoid tissues (He et al., 2016; Im et al., 2016; Im et al., 2020) and integrins are often associated with cell migration, we wondered whether TGF-β controlled the retention of Tcf-1⁺ cells

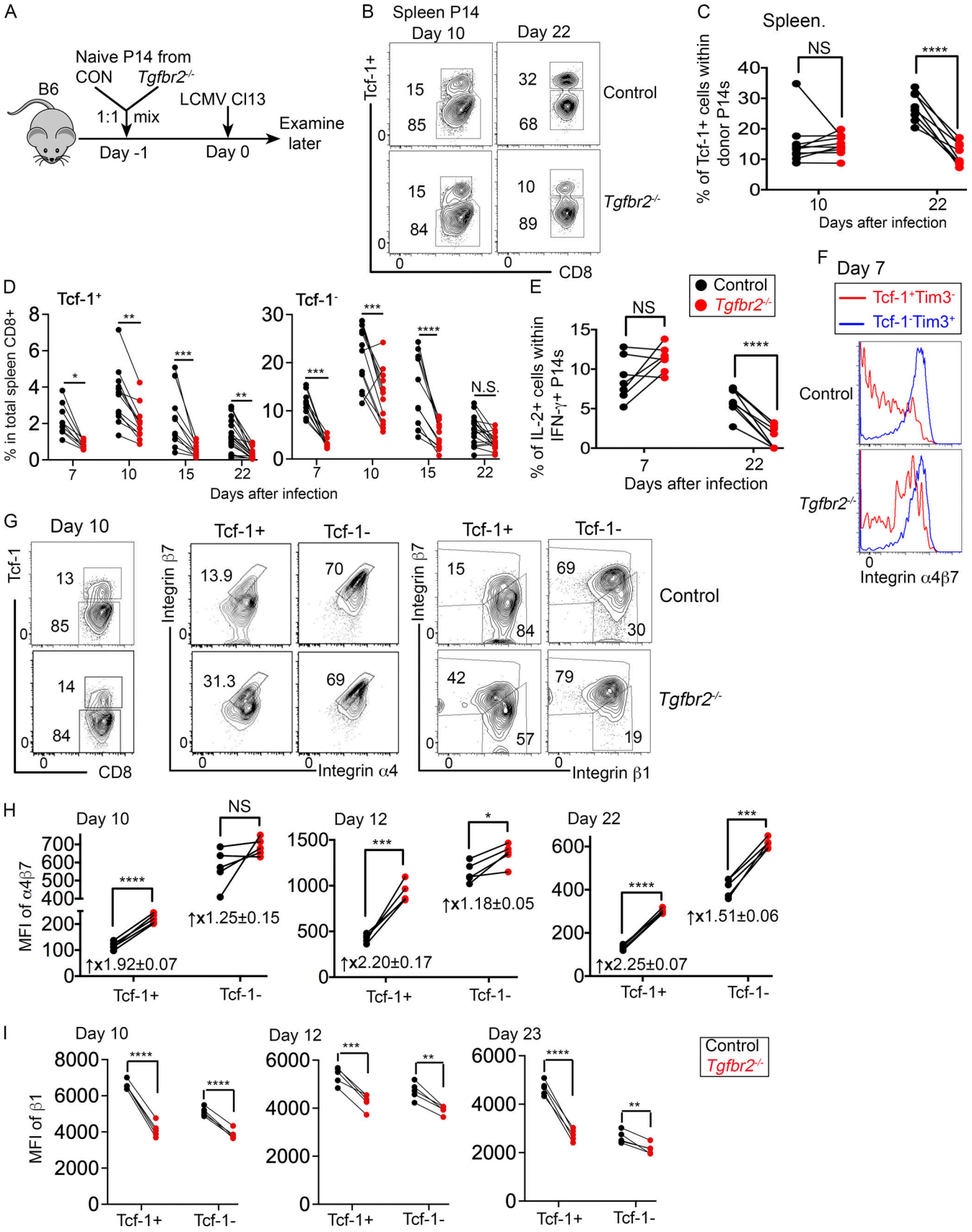

Figure 1. **TGF-β promotes stem-like CD8⁺ T cells during chronic viral infection. (A)** Experimental design. **(B)** At indicated days after infection, representative FACS profiles of pre-gated donor P14 T cells are shown (six repeats, *n* = 4–5/each). **(C)** The percentage of Tcf-1⁺ cells in P14 T cells is shown. **(D)** The

percentage of Tcf-1⁺ (left) and Tcf-1⁻ (right) donor P14 T cells in total splenic CD8⁺ T cells is shown. **(E)** The percentage of IL-2 producing cells in IFN-γ⁺ P14 T cells is shown. **(F and G)** Day 7 (F) and day 10 (G) after infection, representative FACS profiles of pre-gated Tcf-1⁺ and Tcf-1⁻ P14 T cells are shown (three repeats, *n* = 4–5/each). **(H and I)** Mean fluorescence intensity (MFI) of integrin α4β7 (H) and MFI of integrin β1 (I) on Tcf-1⁺ and Tcf-1⁻ P14 cells are shown. The number in H was calculated as the ratio of MFIα4β7 on *Tgfbr2*$^{-/-}$ over MFIα4β7 on co-transferred control P14s in each recipient mouse. Each pair of symbols in C–E, H, and I represents the results from an individual recipient. Combined results from three (C, total *n* = 8–10/time point), six (D, *n* = 10–18/time point), three (E, *n* = 7–9/time point), and three (H and I, *n* = 5/time point) independent experiments are shown. *, P < 0.05; **, P < 0.01; ***, P < 0.001; and ****, P < 0.0001 by paired Student's *t* test for each time point.

inside lymphoid tissues via manipulating the expression of integrins. To this end, we compared Tcf-1⁺ P14 donor T cells isolated from the spleen and peripheral blood of the same animals. At early stage after LCMV Cl13 infection, although highly enriched in lymphoid follicles, a clear Tcf-1⁺ stem-like P14 subset was detected in the peripheral blood (Fig. 2 A). Interestingly, we observed a stepwise reduction of Tcf-1⁺ subset in the blood as infection progressed (Fig. 2 B). Blood Tcf-1⁺ subset was composed of a much higher portion of *Tgfbr2*$^{-/-}$ cells compared with both spleen red pulp and spleen follicles (Fig. 2 C), demonstrating that Tcf-1⁺ cells were more likely to enter the circulation in the absence of TGF-β signaling. Although we observed a subtle increase of *Tgfbr2*$^{-/-}$ Tcf-1⁺ cells in spleen red pulp compared with lymphoid follicles, the difference did not reach statistical significance (Fig. 2 C). Furthermore, circulating WT Tcf-1⁺ subset carried significantly higher portion of β1 β7 double positive cells than their splenic counterparts (Fig. 2, D–E). *Tgfbr2*$^{-/-}$ Tcf-1⁺ subset carried increased population of β1 β7 double-positive cells in both blood and spleen (Fig. 2, D and E). Together, consistent with altered integrin expression pattern, TGF-β promotes the retention of stem-like CD8⁺ T cells inside lymphoid tissues and limits their egress into the circulation.

To further evaluate the role of TGF-β during chronic LCMV infection, we examined the distribution of TGF-β–producing cells in the spleen by immunohistochemistry (Fig. S2 F). We could detect TGF-β–producing cells both inside and outside lymphoid follicles. Together with the recent findings that stem-like CD8⁺ T cells carried higher levels of TGF-β–activating integrin αvβ8 (Gabriel et al., 2021), it is likely that there is a TGF-β–rich microenvironment for stem-like T cells inside lymphoid organs during chronic viral infection.

Enhanced differentiation of transitional subsets in the absence of TGF-β

It has been demonstrated that both stem-like and terminally exhausted CD8⁺ T cells carry tissue-resident T cell marker CD69 and are not circulating. Only transitional subsets are migratory (Beltra et al., 2020). Given our findings that *Tgfbr2*$^{-/-}$ stem-like

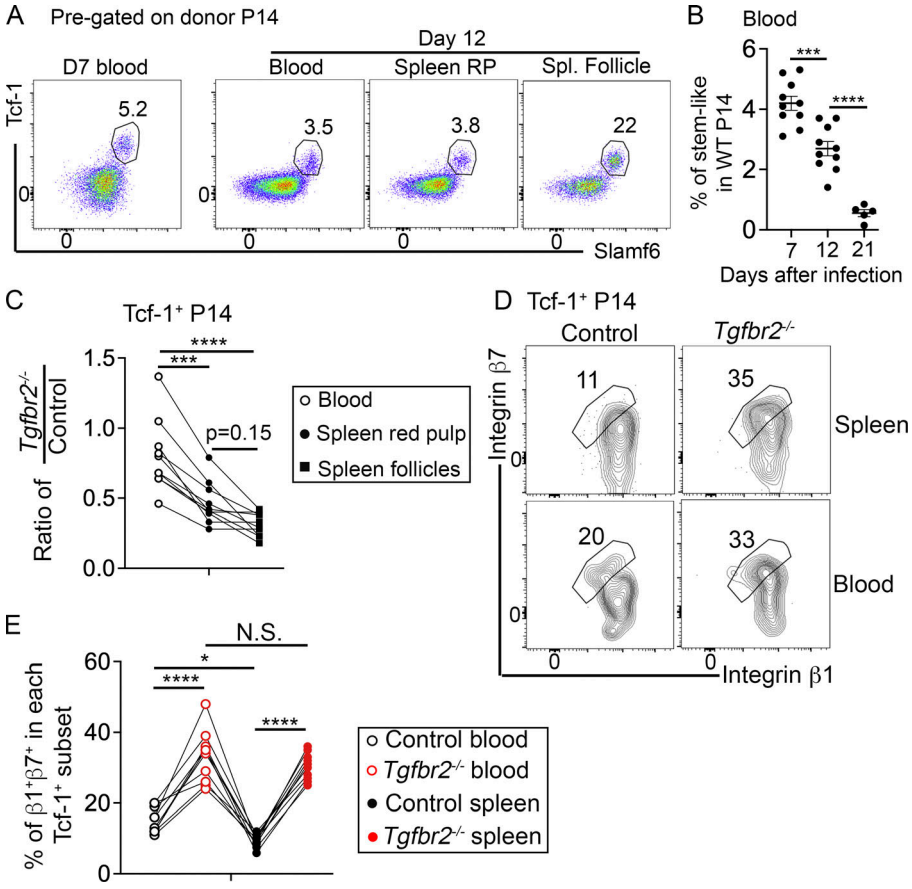

Figure 2. **TGF-β controls the lymphoid tissue retention of Tcf-1⁺ CD8⁺ T cell subset.** Same experimental setup as in Fig. 1. **(A)** Day 7 and day 12 after infection, representative FACS profiles of pre-gated donor WT P14 T cells are shown (two independent repeats, *n* = 4–5/each). **(B)** The percentage of Tcf-1⁺Slamf6⁺ subset in WT P14 T cells from peripheral blood is shown. **(C)** Day 12 after infection, the ratio of *Tgfbr2*$^{-/-}$ Tcf-1⁺ over control Tcf-1⁺ P14 T cells from different tissues is shown. **(D)** Representative FACS profiles of pre-gated Tcf-1⁺ P14 T cells are shown (two independent repeats). **(E)** The percentage of β1⁺β7⁺ cells in each Tcf-1⁺ subset is shown. Each symbol in B and each group of connected symbols in C and E represents the results from an individual recipient mouse. Pooled results from five (B, total *n* = 5–10) or two (C and E, total *n* = 10) independent experiments are shown. *, P < 0.05; ***, P < 0.001; and ****, P < 0.0001 by ordinary one-way ANOVA.

subset exhibited defective maintenance and enhanced circulation, we wondered whether TGF-β suppressed the differentiation of transitional CD8⁺ subsets during chronic viral infection. To this end, we examined the four subsets of exhausted CD8⁺ T cells defined by the expression of Tcf-1 and CD69, i.e., Tcf-1⁺CD69⁺ resident stem, Tcf-1⁺CD69⁻ transitional stem, Tcf-1⁻CD69⁻ migratory effector, and Tcf-1⁻CD69⁺ terminal effector (red pulp resident). As shown in Fig. 3, A and B, while both Tcf-1⁺CD69⁺ tissue-resident stem-like and terminally exhausted Tcf-1⁻CD69⁺ subsets were significantly reduced, Tcf-1⁻CD69⁻ migratory effectors were dramatically enhanced in the absence of TGF-β signaling. Transitional stem-like Tcf-1⁺CD69⁻ subset was slightly reduced in *Tgfbr2*$^{-/-}$ cells. Intravascular anti-CD8 labeling separates splenic CD8⁺ T cells into red pulp and lymphoid follicle compartments. We found that Tcf-1⁺ subsets, especially transitional Tcf-1⁺CD69⁻ subset exhibited enhanced access to intravascular antibody labeling without TGF-β signaling (Fig. 3, C and D), suggesting that *Tgfbr2*$^{-/-}$ Tcf-1⁺ T cells were more likely to localize outside lymphoid follicles. As expected, both Tcf-1⁻CD69⁻ and Tcf-1⁻CD69⁺ were largely confined to the red pulp in the presence and absence of TGF-β signaling (Fig. 3, C and D). Consistent with the results from early time points (Figs. 1 and 2), *Tgfbr2*$^{-/-}$ cells carried significantly increased populations of β1β7 double positive cells at day 22 after infection (Fig. 3 E). Importantly, the impacts of TGF-β signaling on β1β7–co-expressing population were much more dramatic for migratory subsets (CD69⁻ cells, including both Tcf-1⁺CD69⁻ and Tcf-1⁻CD69⁻) compared with resident counterparts (CD69⁺ cells, including both Tcf-1⁺CD69⁺ and Tcf-1⁻CD69⁺; Fig. 3 E).

CX3CR1 has been established as a convenient marker to define migratory effector CD8⁺ T cells with superior cytotoxic activity (Zander et al., 2019). Consistently, in WT cells, CX3CR1 expression was largely restricted to Tcf-1⁻ CD69⁻ cells (Fig. 3, F and G). In *Tgfbr2*$^{-/-}$ cells, the expression of CX3CR1 was further enhanced on Tcf-1⁻ CD69⁻ subset and significantly increased on terminally exhausted Tcf-1⁻ CD69⁺ subset (Fig. 3, F and G). In Fig. 1 E, we have demonstrated altered cytokine production in *Tgfbr2*$^{-/-}$ P14 T cells. Further, it is generally accepted that TGF-β signaling directly suppresses CD8⁺ effector functions. To accurately access the role of TGF-β in CD8⁺ effector function during chronic viral infections, we incorporated Tcf-1 staining to separate stem-like vs. non-stem P14 T cells. Interestingly, when separating Tcf-1⁺ vs. Tcf-1⁻ subsets, at day 22 after infection, we did not detect any significant changes in both cytokine production and granzyme expression in the presence vs. absence of TGF-β receptor (Fig 4, A–C). These results suggest that TGF-β does not directly control CD8 effector function at late stages during chronic viral infection, but instead regulates Tcf-1⁺→Tcf-1⁻ cell differentiation. Consistent with this notion, when examining exhaustion markers (Tox and Tim-3) on Tcf-1⁺ cells, *Tgfbr2*$^{-/-}$ cells exhibited comparable expression levels as WT controls (Fig. 4, D–F). We did detect a reduction of Tox expression in *Tgfbr2*$^{-/-}$ Tcf-1⁻ subset (Fig. 4, D and E), presumably due to decreased Tcf-1⁻CD69⁺ terminally exhausted subset in the absence of TGF-β receptor (Fig. 3, A and B).

To directly test whether TGF-β inhibits the differentiation from Tcf-1⁺ to Tcf-1⁻ CD8⁺ T cells, we performed a stem-like CD8⁺ adoptive transfer assay. Briefly, congenically marked WT and *Tgfbr2*$^{-/-}$ mice were infected by LCMV Cl13. 2 wk later, stem-like CD8⁺ T cells were FACS sorted and adoptively transferred into infection-matched WT mice (Fig. 4 G). 7 d after transfer, we did not detect significant difference in the population size between WT and *Tgfbr2*$^{-/-}$ donor cells (Fig. 4 H). In contrast, significantly increased CX3CR1⁺ cells were observed in *Tgfbr2*$^{-/-}$ donors (Fig. 4, I and J). A consistent trend of reduction was detected for Tcf-1⁺ subset (Fig. 4, I and J).

Together, in *Tgfbr2*$^{-/-}$ CD8⁺ T cells, reduced Tcf-1⁺ stem-like population is associated with enhanced differentiation into transitional subsets and elevated circulation.

α4 integrin blocking promotes Tcf-1⁺ maintenance

To test whether there was a causal link between altered integrin expression, defective Tcf-1⁺ cells and enhanced differentiation into transitional effectors in *Tgfbr2*$^{-/-}$ CD8⁺ T cells, we blocked α4 integrins starting after the early stages of the infection (Fig. 5 A). Percentage-wise, 12 d of blocking significantly rescued *Tgfbr2*$^{-/-}$ Tcf-1⁺ subset (Fig. 5, C–E; and Fig. S4 A). Further, blockade of α4 integrins rapidly boosted Tcf-1⁺ cells even in WT cells (Fig. 5, C and D). To be noted, at the dose of blocking antibody we were using, the blocking was not complete as we could still detect slightly enhanced expression of integrinα4β7 on *Tgfbr2*$^{-/-}$ P14 T cells (Fig. S4 B). In addition, α4 integrin blocking did not significantly interfere with viral clearance (Fig. 5 B), which allowed us to avoid confounding factors when examining the differentiation of P14 T cells. Consistent with the percentage, when total population size was considered, α4 integrin blocking did not impact Tcf-1⁻ subset while it significantly boosted Tcf-1⁺ subset, especially for *Tgfbr2*$^{-/-}$Tcf-1⁺ cells (Fig. 5 F). One step further, we asked whether α4 integrin blocking could boost Tcf-1⁺ cells when given at a later stage. Indeed, when blocking was initiated on day 25 after infection, we could detect a similar and significant enhancement of Tcf-1⁺ subsets 5 d later (Fig. 5, G and H). Together, we have demonstrated that altered expression of α4 integrins was at least partially responsible for the defective maintenance of Tcf-1⁺ stem-like cells in the absence of TGF-β signaling.

α4 Integrin blocking leads to accumulation of migratory effectors

So far, we have demonstrated that TGF-β controls α4 integrin expression and boosts Tcf-1⁺ subset during chronic viral infection possible via enforcing lymphoid tissue retention of stem-like subset. In other words, the differentiation of Tcf-1⁺ stem-like subset is tightly associated with the appearance of migratory effectors, which require α4 integrin to leave lymphoid tissues. If this was true, we expected that α4 integrin blocking would not only boost Tcf-1⁺ stem-like T cells but would also trap more migratory effectors inside the spleen. As shown in Fig. 6 A, when examining CX3CR1 and CD69 together, we could identify two subsets of P14 T cells, i.e., CX3CR1⁺CD69^{lo} migratory and CX3CR1^{lo}CD69⁺ resident ones. For WT Tcf-1⁺ cells, the vast majority was CX3CR1^{lo}CD69⁺ resident cells while for WT Tcf-1⁻ ones, both CX3CR1⁺CD69^{lo} migratory and CX3CR1^{lo}CD69⁺ resident cells were readily detectable (Fig. 6 A, left column). For *Tgfbr2*$^{-/-}$ P14 T cells, there was a significant increase in CX3CR1⁺CD69^{lo} migratory subset, especially for Tcf-1⁻ subset

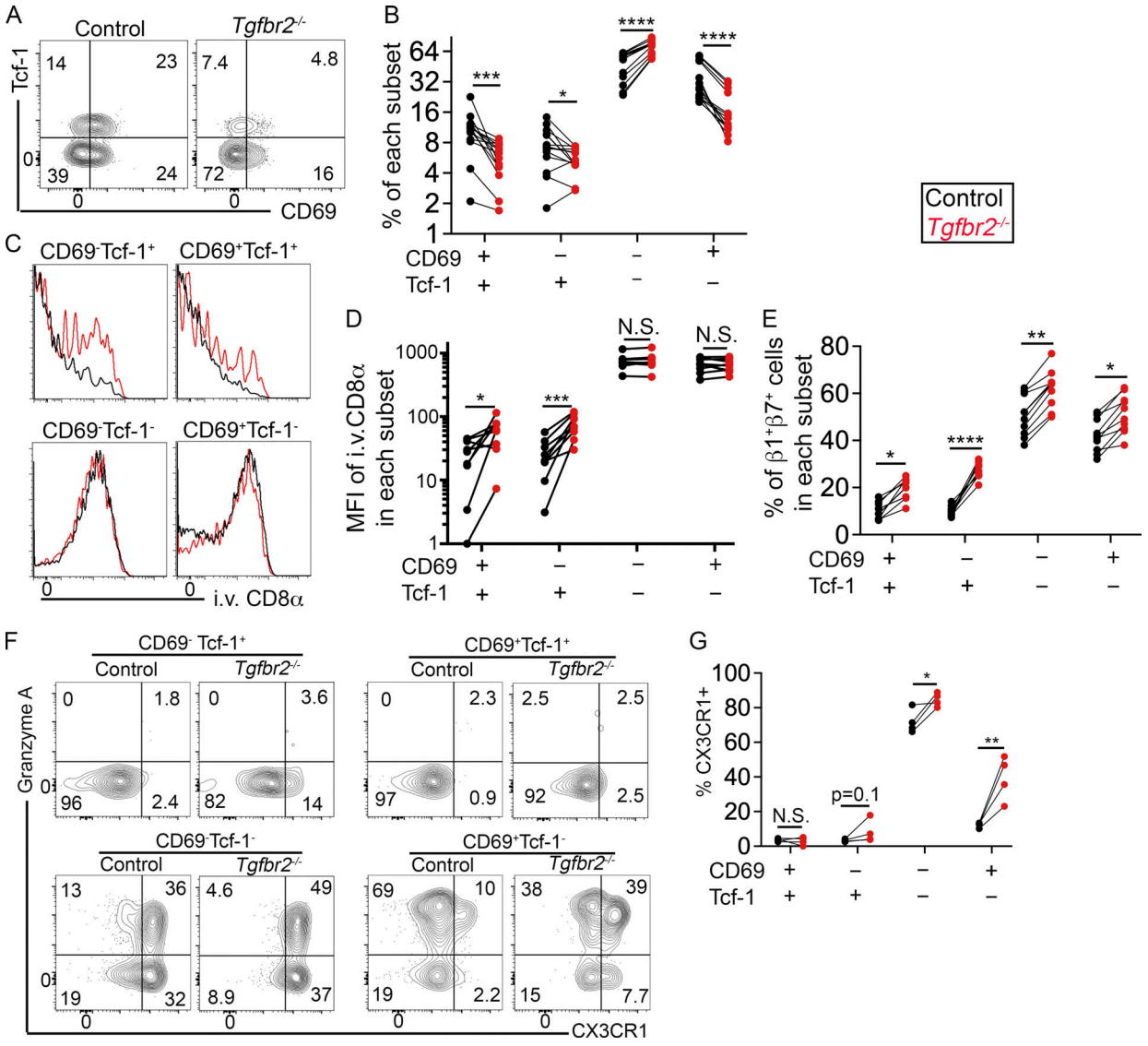

Figure 3. **TGF-β suppresses the differentiation of transitional subsets of CD8⁺ T cells. (A)** Same experimental setup as in Fig. 1. Day 21–23 after infection, representative FACS profiles of pre-gated donor P14 T cells isolated from the spleen (three independent repeats). **(B–G)** Characterization of the four P14 subsets defined by the expression of Tcf-1 and CD69. The percentage of each subset in total P14 T cells (B), intravascular anti-CD8α labeling in each subset (C and D), and the percentage of β1⁺β7⁺ cells in each subset (E) are shown. **(F)** Representative FACS profiles to show the expression of CX3CR1 and Granzyme A in each subset of P14 T cells. **(G)** The percentage of CX3CR1⁺ cells in each subset is shown. Each pair of symbols in B, D, E, and G represents the results from an individual recipient mouse. Pooled or representative results from two (C–E, *n* = 10; F and G, *n* = 4) or three (A and B, *n* = 14) independent experiments are shown. *, P < 0.05; **, P < 0.01; ***, P < 0.001; and ****, P < 0.0001 by ordinary one-way ANOVA or Student's *t* test.

(Fig. 6 A). In the presence of α4 integrin blocking, we detected a slight, but often significant increase of CX3CR1⁺CD69^{lo} migratory cells and a consistent reduction of CD69⁺ resident cells (Fig. 6, A–D). Importantly, α4 blocking had minimal impacts on the effector functions of P14 T cells when Tcf-1⁺ and Tcf-1⁻ subsets were separately examined (Fig. 6, E–G).

To further strengthen this conclusion that α4 integrin blocking boosts stem-like T cells via suppressing T cell migration, we FACS-sorted Slamf6⁺ vs. Slamf6⁻ P14 T cells and cultured sorted cells with GP_{33-41} peptide-pulsed splenocytes in the presence or absence of α4 blocking antibody (Fig. S4 C). 4 d after culture, as expected, Slamf6⁻ input cells remained Slamf6⁻Tcf-1⁻ while Slamf6⁺ input ones differentiated into both Tcf-1⁺ and Tcf-1⁻ cells. Importantly, α4 integrin blocking did not impact Tcf-1⁺→Tcf-1⁻ differentiation in this in vitro setting when cell migration was not involved (Fig. S4 D).

Together, these results strongly support the conclusion that α4 integrin blocking promotes Tcf-1⁺ stem-like subset via suppressing T cell migration.

α4 Integrin blocking promotes the retention of stem-like T cells inside lymphoid follicles

To test whether α4 integrin blocking directly impacts lymphoid tissue retention of stem-like CD8⁺ T cells, we shortened the duration of the treatment. As illustrated in Fig. 7 A, mice were examined after two injections of α4 blocking antibody.

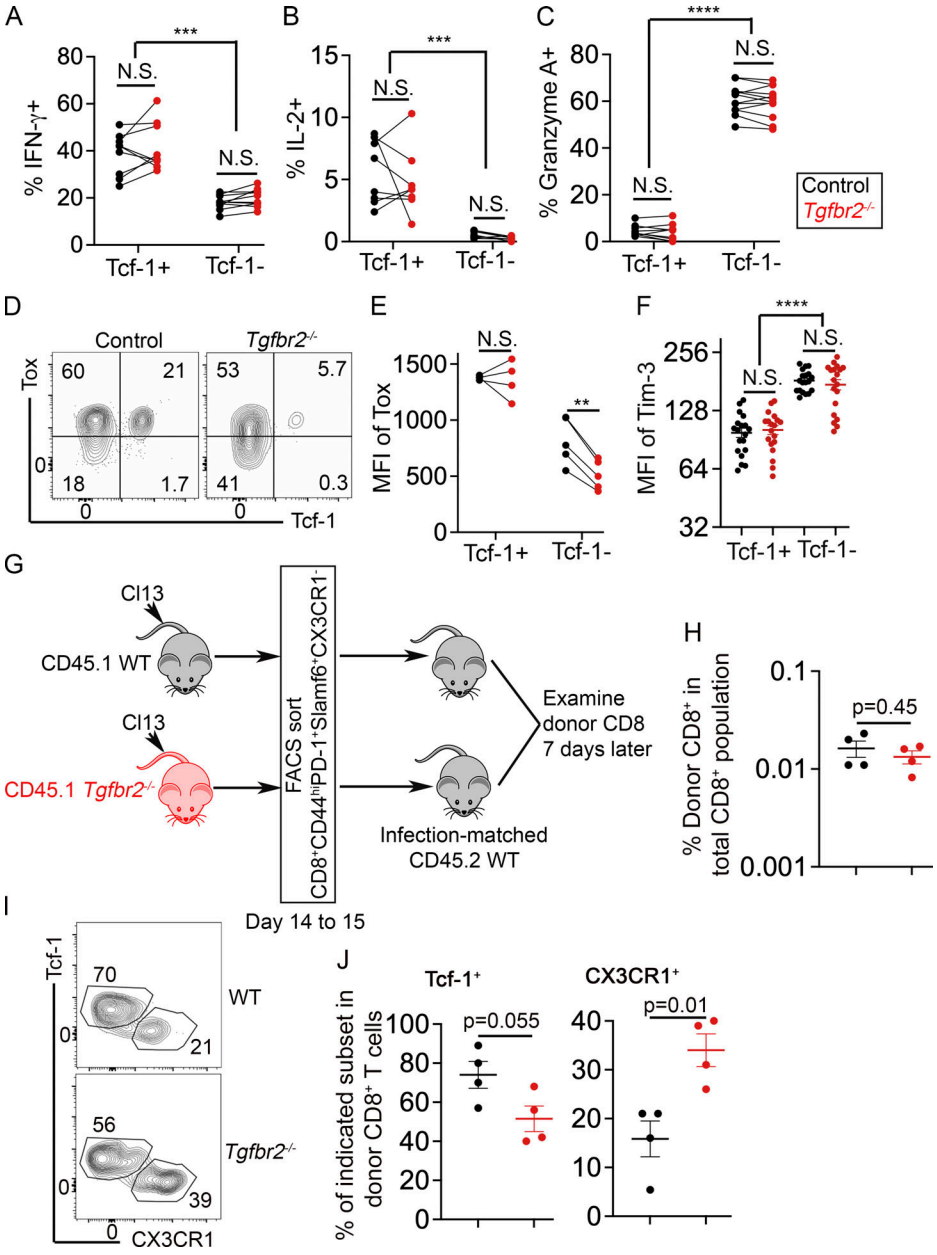

Figure 4. **TGF-β suppressed the differentiation, but not the effector functions of Tcf-1⁺ stem-like T cells**. Similar experimental setup to Fig. 1. **(A–C)** Day 22 after infection, the percentage of IFN-γ⁺ (A), IL-2⁺ (B), and granzyme A⁺ (C) cells in Tcf-1⁺ and Tcf-1⁻ subsets of donor P14 T cells are shown. **(D)** Representative FACS profiles to show the expression of Tox. **(E)** MFI of Tox in Tcf-1⁺ and Tcf-1⁻ subsets are shown. **(F)** MFI of Tim-3 is shown. **(G)** Experimental setup for H–J. **(H)** The percentage of donor CD8⁺ T cells in the total CD8⁺ population is shown. **(I)** Representative FACS profiles of pre-gated donor CD8⁺ T cells are shown. **(J)** The percentage of Tcf-1⁺ (left) and CX3CR1⁺ (right) cells in donor CD8⁺ T cells are shown. Each pair of symbols in A–D, and each symbol in E, H, and J represents the results from an individual recipient mouse. Pooled results from two (A–C, n = 8–12; D and E, n = 5; H–J, n = 4/each) and five (F, n = 19) independent experiments are shown. **, P < 0.01; ***, P < 0.001; and ****, P < 0.0001 by ordinary one-way ANOVA (A–F) or Student's t test (H–J).

Consistent with previous findings (Im et al., 2016), stem-like CD8⁺ T cells were highly enriched in the lymphoid follicles (Fig. 7, B and C). Briefly, α4 integrin blockade dramatically enhanced stem-like CD8⁺ T cells, especially in the lymphoid follicle compartment of the spleen (Fig. 7, B and C). When total cell population was examined, shortened α4 blocking significantly promoted *Tgfbr2*$^{-/-}$ stem-like subset, but not Tcf-1⁻ subsets (Fig. 7 D). We could detect reduced CD69 expression after α4 blocking (Fig. 7 E), suggesting the trapping of CD69⁻ migratory cells. Interestingly, at this early time point, we did observe increased effector function for *Tgfbr2*$^{-/-}$ cells (i.e., granzyme A and IFN-γ). But CD8⁺ effector functions were not affected by α4 integrin blocking (Fig. 7, F–H). Together, blocking α4 integrins significantly improves the lymphoid tissue retention and maintenance of stem-like CD8⁺ T cells in the absence of TGF-β signaling.

To further test the possibility that promoting lymphoid tissue retention would promote stem-like T cells, infected mice were

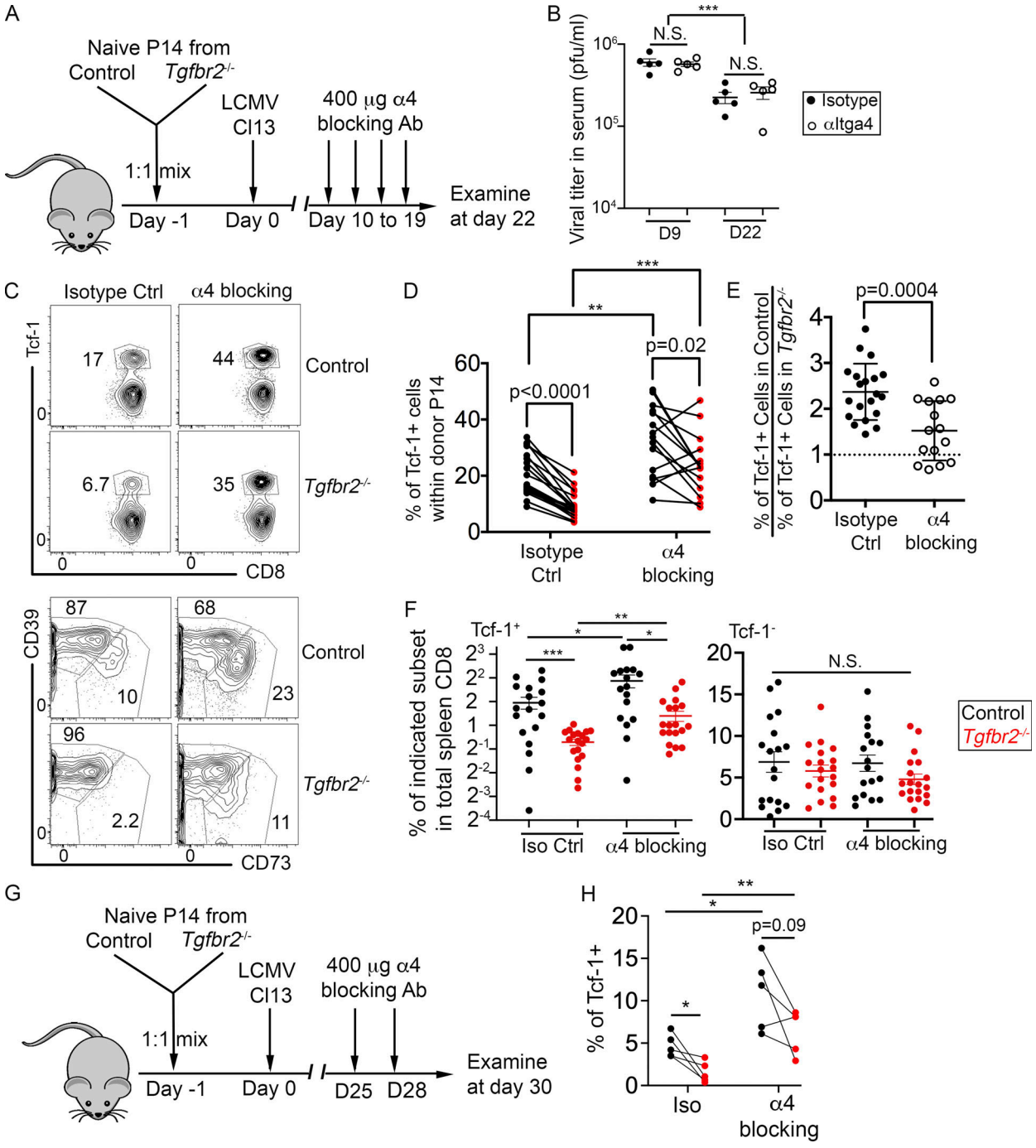

Figure 5. **Blocking integrin α4 partially corrects the defective maintenance of *Tgfbr2*$^{-/-}$ Tcf-1^{+} CD8^{+} T cells. (A)** Experimental design. Same P14 co-transfer and LCMV infection setup as in Fig. 1. Starting from day 10 after infection, integrin α4 blocking antibody was administrated every 3 d and examined on day 22. **(B)** The virus titer in the serum before (d9) and after (d22) αItga4 blocking are shown. **(C)** Representative FACS profiles of pre-gated donor splenic P14 T cells are shown. **(D)** The percentage of Tcf-1^{+} cells among P14 T cells is shown. **(E)** The ratios of Tcf-1^{+} percent in control P14s over Tcf-1^{+} percent in *Tgfbr2*$^{-/-}$ P14s are shown. **(F)** The percentage of Tcf-1^{+} (left) and Tcf-1^{-} (right) donor P14 T cells in total splenic CD8^{+} population are shown. **(G)** Experimental design for delayed integrin α4 blocking. **(H)** The percentage of Tcf-1^{+} subset in donor P14 T cells at day 30 after infection in the presence or absence of delayed α4 blocking. Each pair of symbols in D and H, and each symbol in B, E, and F represent the results from an individual mouse. Representative or pooled results from five independent experiments are shown in (C–F; n = 15–20). Pooled results from two independent experiments are shown in B (n = 5/each) and H (n = 5/each). *, P < 0.05; **, P < 0.01; and ***, P < 0.001 by Student's t test in D, E, and H, or by ordinary one-way ANOVA in B and F.

treated with FTY720, which is a potent inhibitor of lymphocyte egress (illustrated in Fig. S5 A). FTY720 treatment leads to substantial improvement of Tcf-1^{+} population in both WT and *Tgfbr2*$^{-/-}$ cells (Fig. S5 B). Thus, lymphoid tissue retention promotes the maintenance of stem-like CD8^{+} T cells. To further validate our findings that TGF-β promotes stem-like CD8^{+} T cells via enhancing their lymphoid tissue retention and residency, we examined the transcriptional profiles of WT

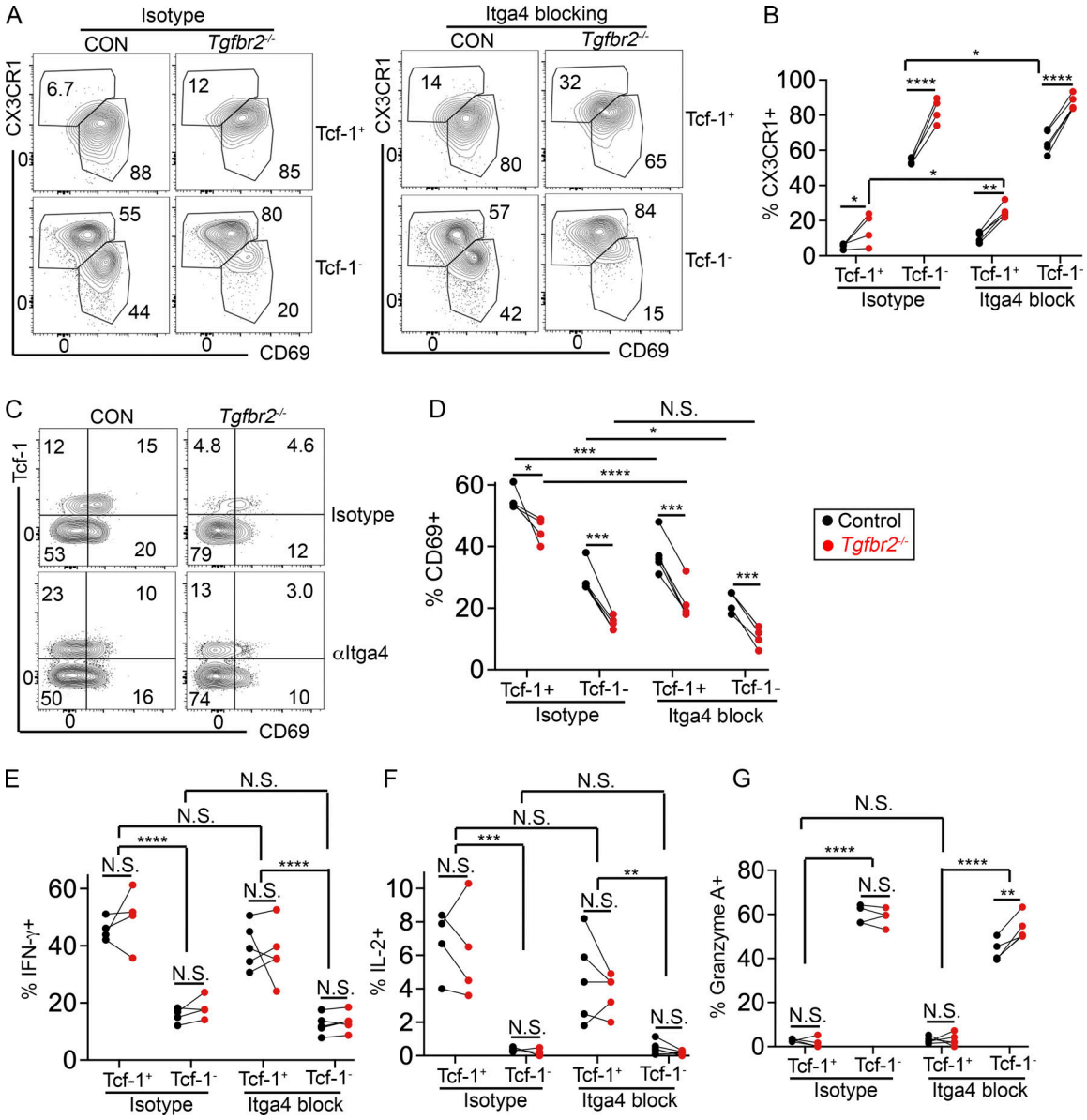

Figure 6. **Integrin α4 blocking traps migratory cells and inhibits the differentiation of stem-like CD8⁺ T cells.** Similar experimental setup to Fig. 5 A. **(A)** Representative FACS profiles of pre-gated Tcf-1⁺ (upper) and Tcf-1⁻ (lower) P14 T cells to show the expression of CX3CR1 and CD69. **(B)** The percentage of CX3CR1⁺ cells in Tcf-1⁺ and Tcf-1⁻ P14s are shown. **(C)** Representative FACS profiles of donor P14 T cells are shown. **(D)** The percentage of CD69⁺ in Tcf-1⁺ and Tcf-1⁻ P14s are shown. **(E–G)** The percentage of IFN-γ⁺ (E), IL-2⁺ (F), and granzyme A⁺ (G) cells in Tcf-1⁺ and Tcf-1⁻ P14s are shown. Each pair of symbols in B, D–F, and G represents the results from an individual recipient. Representative or pooled results from two independent experiments are shown (n = 4–5/each). *, P < 0.05; **, P < 0.01; ***, P < 0.001; and ****, P < 0.0001 by ordinary one-way ANOVA.

and *Tgfbr2*$^{-/-}$ P14 T cells. Briefly, WT and *Tgfbr2*$^{-/-}$ donor P14 T cells were FACS sorted into four subsets based on the expression of Slamf6 and CD69. Taking advantage of established circulating vs. resident core signatures of memory T cells (Milner et al., 2017), we found that most *Tgfbr2*$^{-/-}$ subsets carried significantly defective resident signatures (Fig. S5 D). CD69⁺ subsets of exhausted CD8⁺ T cells have been demonstrated to carry tissue resident features (Beltra et al., 2020). Interestingly, in the absence of TGF-β receptor, both Slamf6⁺CD69⁺ and Slamf6⁻CD69⁺ resident subsets harbored significantly increased circulating T cell signature (Fig. S5 C). These results further strengthen our findings that TGF-β–dependent lymphoid residency is an integrated component of CD8⁺ T cell biology during chronic viral infection.

Discussion

Together, we have demonstrated that TGF-β signaling suppresses the differentiation of stem-like CD8⁺ T cells into transitional subsets partially via controlling the expression of α4 integrins, limiting their egress into the circulation and enhancing their lymphoid tissue retention. Our results suggest a model that the migration out of lymphoid environment is coupled with further differentiation of stem-like CD8⁺ T cells. TGF-

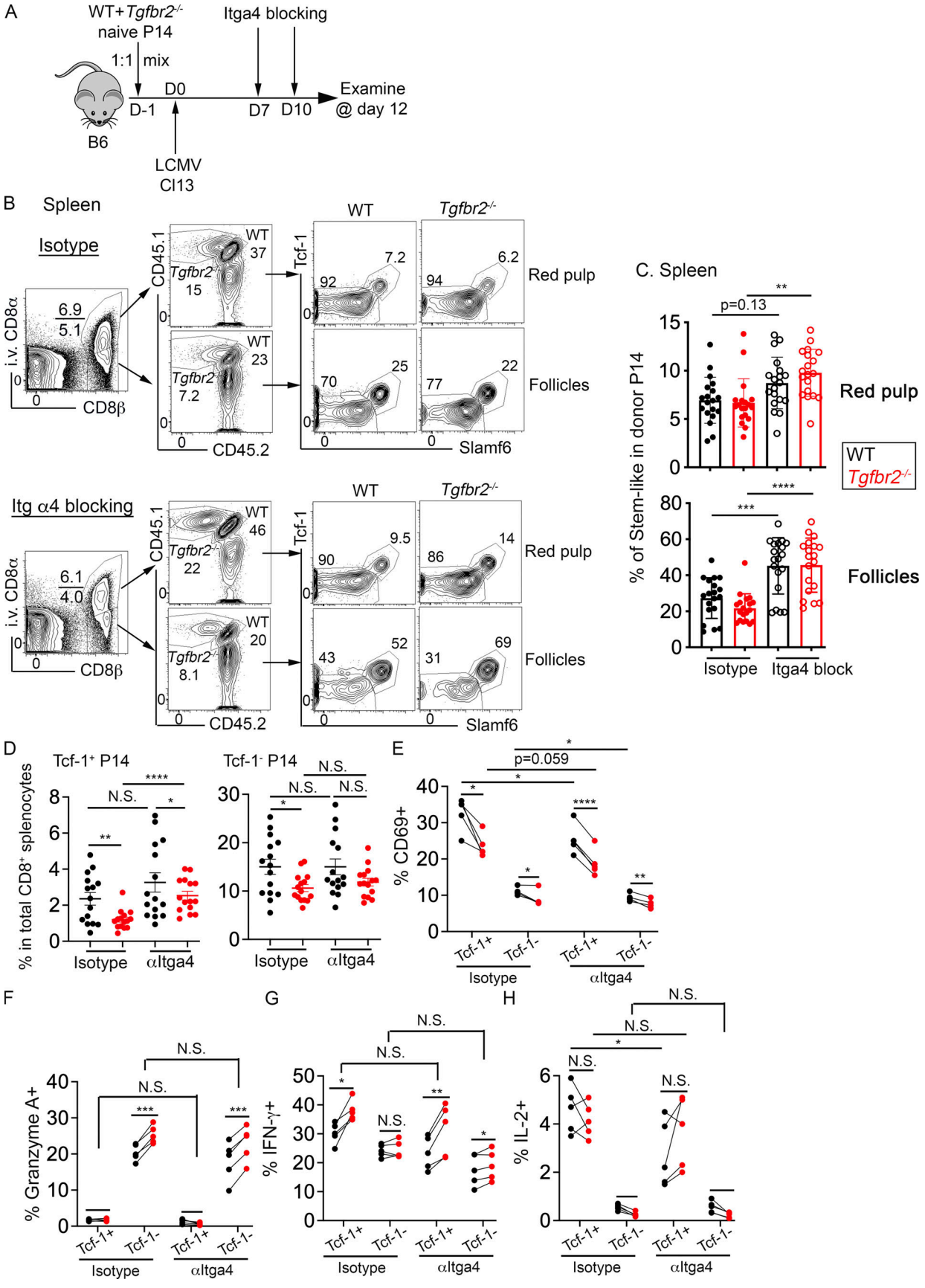

Figure 7. **Blocking α4 integrins enhances lymphoid tissue retention of stem-like CD8⁺ T cells. (A)** Experimental design. Same P14 co-transfer and LCMV infection setup as in Fig. 1. On day 7 and 10 after infection, integrin α4 blocking antibody was administrated and examined on day 12. **(B)** Representative FACS

profiles of splenic lymphocytes are shown. **(C)** The percentage of stem-like subset in P14 T cells located in red pulp (upper) and follicles (lower) is shown. **(D)** The percentage of Tcf-1$^+$ (left) and Tcf-1$^-$ (right) donor P14 T cells in total splenic CD8$^+$ population is shown. **(E)** The percentage of CD69$^+$ in Tcf-1$^+$ and Tcf-1$^-$ P14s is shown. **(F–H)** The percentage of granzyme A$^+$ (F), IFN-γ$^+$ (G), and IL-2$^+$ (H) cells in Tcf-1$^+$ and Tcf-1$^-$ P14s is shown. Each pair of symbols in E–H, and each symbol in C and D represents the results from an individual recipient. Representative or pooled results from four (B–D, n = 15–19/each) or two (E–H, n = 5) independent experiments are shown. *, P < 0.05; **, P < 0.01; ***, P < 0.001; and ****, P < 0.0001 by ordinary one-way ANOVA.

β promotes lymphoid tissue retention and therefore inhibits the effector differentiation of stem-like CD8$^+$ T cells. A recent publication has demonstrated that TGF-β signaling inhibits mTOR to preserve cellular metabolism and maintenance of stem-like T cells during chronic viral infection (Gabriel et al., 2021), which provides elegant evidence that the differentiation of stem-like T cells is controlled by a unique metabolic program. Our results provide another perspective linking TGF-β signaling with stem-like T cells via controlling the retention and localization of stem-like T cells inside lymphoid environment. Our results demonstrate that manipulating the migration and residency of stem-like T cells is sufficient to control their differentiation. Considering the recent evidence that TGF-β-controlled mitochondrial metabolism is required for tissue-resident memory T cell (T_{RM} cell) differentiation (Borges da Silva et al., 2020), it will be interesting to examine whether TGF-β–dependent metabolic program is directly connected with TGF-β–controlled resident program for stem-like T cells in the future.

TGF-β cytokines are secreted as inactive latent forms. Integrin αvβ6 and αvβ8 can activate TGF-β. Gabriel et al. have demonstrated that Tcf-1$^+$ stem-like CD8$^+$ T cells express higher levels of αvβ8 during chronic viral infection, which may partially explain how to maintain a TGF-β–rich microenvironment around stem-like T cells (Gabriel et al., 2021). Our findings demonstrate that TGF-β–controlled integrin α4β7 and α4β1 are essential components of a larger tissue resident program, which helps stem-like T cells to be maintained inside the lymphoid microenvironment. Lymphoid follicles may provide a critical shield from inflammatory insults. Further into the biology of integrins on T cells, it remains unknown whether integrin αvβ8 directly controls the migration of stem-like T cells in addition to TGF-β activation. It is interesting to note that both αv and α4 integrin can form heterodimer with integrin β1 (Hynes and Naba, 2012). Whether this potential competition has any functional consequence in stem-like T cells is unknown.

Considering the well-established role of TGF-β in T_{RM} cell differentiation following acute infections (Casey et al., 2012; Liao et al., 2021; Mackay et al., 2013; Sheridan et al., 2014; Zhang and Bevan, 2013), our results provide evidence that there is a general requirement of TGF-β signaling to maintain tissue-resident phenotypes regardless of acute or chronic infection settings. Consistently, global transcriptional analysis from the accompanying publication by Hu et al. (2022) and our own RNA sequencing (RNA-seq) analysis has demonstrated that *Tgfbr2*$^{-/-}$ CD8$^+$ T cells carry reduced residency signatures and enriched circulating signatures. Thus, in addition to α4 integrins, TGF-β may help stem-like CD8$^+$ T cells establish tissue residency–related transcriptional programs.

Importantly, during chronic LCMV infection, stem-like T cells gradually establish T_{RM} cell program in lymphoid tissues, consistent with stepwise reduction of circulating stem-like T cells (Fig. 2 B), which also explains why TGF-β is preferentially required for the later stages of LCMV infection. Thus, stem-like CD8$^+$ T cells progress along the TGF-β–dependent T_{RM} cell pathway during chronic antigen exposure.

In spite of these similarities, it is noteworthy to point out that there are clear differences between stem-like CD8$^+$ T cells in chronic infection versus T_{RM} cells generated following acute infection. For example, stem-like CD8$^+$ T cells are Tcf-1$^+$ while T_{RM} cells often downregulate Tcf-1 during differentiation (Liao et al., 2021; Wu et al., 2020). Following chronic viral infection, effector CD8$^+$ T cells (including stem-like subset) do not express CD103, which is a commonly used marker for mucosal T_{RM} cells (Zhang and Bevan, 2013). Together, lymphoid tissue-residency is essential for stem-like CD8$^+$ T cells, which share certain features with T_{RM} cells generated following acute infections. Common mechanisms, such as TGF-β signaling are involved in limiting T cell migration in both acute and chronic infections.

In the absence of TGF-β signaling, the percentage of Tcf-1$^+$ stem-like cell population exhibited a two- to threefold reduction. The magnitude of the reduction was maintained and the total population of *Tgfbr2*$^{-/-}$ P14 T cells was not significantly reduced in our hands (Zhang and Bevan, 2013) or increased at later stages (accompanying publication by Hu et al., 2022). The difference may be due to the fact that we used LCMV Cl13 infection system with CD4 help and therefore viremia is largely controlled at a later stage.

Another key difference between our results and the ones from Hu et al. (2022) is the subset phenotype of Tcf-1$^+$ stem-like T cells. In our resolving chronic infection model (i.e., with CD4 help), virus titer was dramatically reduced at later time points (i.e., around day 20–30) and Tcf-1$^+$ cells can be further divided into CD69$^+$ vs. CD69$^-$ subsets. It is CD69$^-$Tcf-1$^+$ cells directly differentiating into CD69$^-$Tcf-1$^-$ migratory effectors (Beltra et al., 2020). TGF-β mainly controls α4 integrin expression on both CD69$^-$Tcf-1$^+$ and CD69$^-$Tcf-1$^-$ transitional cells and suppresses the migratory capacity of CD69$^-$Tcf-1$^+$ transitional stem subset. In contrast, in life-long viremia model, Tcf-1$^+$ stem-like cells are often uniformly CD69$^+$ and largely tissue-resident with little exchange with the circulation (Im et al., 2020). In this situation, CD69$^+$Tcf-1$^+$ stem-like cells downregulate both CD69 and Tcf-1 to differentiate into transitional and circulating effectors, which is inhibited by TGF-β (accompanying publication by Hu et al., 2022). Together, regardless of resolving vs. life-long viremia, we have demonstrated that TGF-β inhibits the differentiation of Tcf-1$^+$ stem-like CD8$^+$ T cells into transitional states during chronic infection, coinciding with the loss of tissue residency and enhanced migration.

Recently findings in tumor immunotherapies have demonstrated that TGF-β inhibitors are beneficial due to their effects

on tumor stromal compartments (Mariathasan et al., 2018; Tauriello et al., 2018) and CD4+ T cell–mediated blood vasculature remodeling (Li et al., 2020; Liu et al., 2020). Since it is the migratory effector CD8+ T cells, not the stem-like ones carrying most cytotoxic activity (Hudson et al., 2019; Zander et al., 2019), our results suggest that in addition to the stromal compartments and CD4+ T cells, direct targeting TGF-β signaling in CD8+ T cells may promote differentiation from stem-like cells into cytotoxic effectors and therefore contribute to the beneficial effects seen in combined tumor immunotherapies.

Materials and methods

Mice and virus

C57BL/6J (B6) mice were obtained from The Jackson Laboratory and a colony of D^b-GP_{33-41} TCR transgenic (P14) mice was maintained at our specific pathogen–free animal facilities at the University of Texas Health Science Center at San Antonio (San Antonio, TX). All recipient mice were used at 6–10 wk of age and were directly ordered from The Jackson Laboratory. *Tgfbr2*$^{f/f}$ and dLck-cre mice were described before (Zhang and Bevan, 2012). All donor P14 mice have been backcrossed to C57BL/6 background for at least 12 generations. All mice were housed at our specific pathogen–free animal facilities at the University of Texas Health San Antonio. All experiments were done in accordance with the University of Texas Health Science Center at San Antonio Institutional Animal Care and Use Committee guidelines. Mice were infected i.v. by 2 × 10^6 pfu LCMV Clone 13. Viruses were grown and quantified as described (Zhang and Bevan, 2013).

Antibodies and flow cytometry

For in vivo α4 integrin blocking, anti-α4 integrin (PS/2) antibody was from Bio X Cell. Fluorescent dye–labeled antibodies specific for PD-1 (J43), CXCR5 (SPRCL5), CD8β (H35-17.2), CD45.1 (A20), CD45.2 (104), CD8α (53-6.7), CD44 (IM7), CX3CR1 (SA011F11), Granzyme A (GzA-3G8.5), integrin α4β7 (DAPK32), CXCR3 (CXCR3-173), CD39(24DMS1), CD73(TY/11.8), CD62L(MEL-14), Ly6C(HK1.4), CD49d (R1-2), integrin β1 (HMB1-1), integrin β7 (FIB504), IFN-γ (XMG1.2), IL-2 (JES6-5H4), Slamf6 (330-AJ), Tim-3 (RMT3-23), and Tox (TXRX10) were purchased from eBioscience, Biolegend, and Tonbo. Anti-CD16/32 (2.4G2) was produced in the lab and used in all FACS staining as FcR blocker. Anti–Tcf-1 (C63D9) and pSmad2/3 (EBF3R) were from Cell Signaling. Intranuclear staining for Tcf-1 and Tox was performed using a Foxp3 staining buffer set (Tonbo Bioscience). For intracellular cytokine staining, freshly isolated splenocytes were cultured with 0.1 μM GP_{33-41} peptide (AnaSpec) in the presence of Golgi Stop (BD) for 4–5 h at 37°C. After surface staining, IFN-γ and IL-2 were performed using permeabilization buffer (Invitrogen) following fixation. Ghost Dye Violet 510 (Tonbo Bioscience) was used to identify live cells. Washed and fixed samples were analyzed by BD LSRII or BD FACSCelesta and analyzed by FlowJo (TreeStar) software.

Naive T cell isolation and adoptive transfer

Naive CD8+ T cells were isolated from pooled spleen and lymph nodes using MojoSort mouse CD8 T cell isolation kit (Biolegend) following the manufacturer's instructions. During the first step of biotin antibody cocktail incubation, biotin-αCD44 (IM7; Biolegend) was added to label and deplete effector and memory T cells. Isolated naive CD8+ T cells were numerated, 1:1 mixed, 10^4 cells adoptively transferred into each sex-matched unmanipulated B6 recipient via an i.v. route.

Integrin ligand binding assay

As described before (Dimitrov et al., 2019), at indicated time after infection, splenocytes were incubated with 5 μg/ml recombinant mouse ICAM-1-Fc (human IgG; Biolegend), rmMAdCAM-1-Fc (human IgG; R&D Systems), or rmVCAM-1-Fc (human IgG; R&D Systems) in the presence of 0.1 μM GP_{33-41} at 37°C for 5 min followed by surface staining including FITC-donkey anti-human IgG (Jackson ImmunoResearch) on ice and analyzed by flow cytometry.

FTY720 treatment

100 μg/kg body weight FTY720 (Sigma-Aldrich) was injected peritoneally starting from day 10 after Cl13 infection on a daily basis. P14 T cell response was examined 12 d after the initial FTY720 injection.

Integrin α4 blocking

400 μg/mouse anti-integrin α4 antibody (PS/2, Bio X cell) or isotype control antibody was injected peritoneally starting from day 7, 10, or 25 after LCMV Cl13 infection every 3 d. Mice were examined at indicated time points.

Intravascular labeling of CD8+ T cells

3 μg biotin-αCD8α (53-6.7; Tonbo Biosciences) was injected i.v. 5 min before euthanasia. After lymphocyte isolation, fluorescence-labeled streptavidin (Thermo Fisher Scientific) was used during surface staining to identify red pulp–located splenic CD8+ T cells.

H&E staining

At indicated time points after infection, various tissues were dissected and fixed in 10% neutral buffered formalin. All further procedures including paraffin-embedding, sectioning, and H&E staining were performed by UT Health San Antonio pathology core facility.

Immunohistochemistry

To detect LCMV antigen, at indicated time points after infection, livers were snap-frozen in OCT Compound (Thermo Fisher Scientific). At room temperature, 7 μM sections were fixed with 4% paraformaldehyde for 30 min, permeablized by 1% Triton for 20 min, and blocked with 4% FCS/PBS for 20 min. Slides were incubated with anti-LCMV (VL-4; Bio X Cell) followed by second antibody incubation (Peroxydase AffiniPure Goat anti-Rat IgG; Jackson Immuno). After washing, KPL TrueBlue Substrate (Seracare Life Sci.) was applied following the manufacturer's instruction. The slides were counterstained by KPL Contrast RED (Seracare Life Sci.).

To detect TGF-β, at indicated time points after infection, various tissues were dissected and fixed in 10% neutral buffered formalin. All further procedures including paraffin-embedding,

sectioning, immunohistochemistry, and H&E staining were performed by UT Health San Antonio pathology core facility. Briefly, sections were incubated with 5 µg/ml αTGF-β1 (#NBP1-80289; Novus Biologicals) as first antibody, an anti-rabbit IgG-HRP as secondary antibody, and developed with 3,3′-diaminobenzidine substrate.

Stem-like T cell sorting and transfer

WT and *Tgfbr2*$^{-/-}$ mice were infected by LCMV Cl13. Day 14–15 after infection, total CD8$^+$ T cells were enriched from pooled spleen and lymph nodes by depleting CD4$^+$ and CD19$^+$ cells. CD44^{hi}PD-1^{hi}Slamf6$^+$CX3CR1$^-$CD8$^+$ T cells were FACS sorted from enriched cells. 10^5 sorted cells/recipient were adoptively transferred into infected match B6 recipients. Donor CD8$^+$ T cells were examined 7 d later.

RNA-seq analysis

Day 15 after LCMV Cl13 infection, donor WT and *Tgfbr2*$^{-/-}$ P14 T cells were FACS sorted into four subsets based on the expression of Slamf6 and CD69. Total RNA was extracted from sorted cells using the Quick-RNA MiniPrep kit from Zymo Research. Biological independent duplicates were included. RNA-seq analysis was performed by Novogene, and the results can be accessed by GSE206646.

Stem-like T cell in vitro culture

WT P14 T cells were adoptively transferred into B6 mice followed by LCMV Cl13 infection. Day 14 after infection, Slamf6$^+$ and Slamf6$^-$ P14 T cells were FACS sorted from total splenocytes and lymph node cells. Meanwhile, CD8/NK-depleted splenocytes were purified from infection-matched B6 controls. 10^4 sorted P14 T cells were co-cultured with 10^5 CD8/NK-depleted splenocytes in the presence of 1 µM GP_{33-41} + 10 ng/ml IL-2 (Biolegend) with or without 10 µg/ml PS/2 antibody. Live P14 T cells were examined 4 d later by flow cytometry.

Statistical analysis

Ordinary one-way ANOVA or Student's *t* test from Prism 9 was used.

Online supplemental material

Fig. S1 shows defective stem-like CD8$^+$ T cells in the absence of TGF-βR, further supporting the results in Fig. 1, A–E. Fig. S2 shows stem-like T cells in the presence and absence of CD4 help, viral clearance, non-lymphoid tissue pathology, as well as the detection of TGF-β–producing cells during chronic viral infection. Fig. S3 shows integrin ligand binding on donor P14 T cells. Fig. S4 shows the results from lymph node P14 T cells after in vivo α4 integrin blocking as well as the results from in vitro α4 blocking. Fig. S5 shows the results from in vivo FTY720 treatment experiments and bulk RNA-seq experiments.

Acknowledgments

We thank Drs. Rafi Ahmed and Yinghong Hu for suggestions and discussions throughout the project. We thank Karla Gorena and Sebastian Montagnino for FACS sorting.

This work is supported by National Institutes of Health grants AI125701 and AI139721, Cancer Research Institute CLIP program, and the American Cancer Society grant RSG-18-222-01-LIB to N. Zhang. Data were generated in the Flow Cytometry Shared Resource Facility, which is supported by the University of Texas Health Science Center at San Antonio, the Mays Cancer Center National Institutes of Health/National Cancer Institute grant P30 CA054174, and the National Center for Advancing Translational Science, National Institutes of Health, through grant UL1 TR002645.

Author contributions: C. Ma and N. Zhang designed the experiments. C. Ma, W. Liao, Y. Liu, S. Mishra and G. Li performed the experiments. L. Wang performed the RNA-seq experiment. C. Ma, L. Wang, and N. Zhang analyzed the results. X. Zhang, Y. Qiu, and Q. Lu contributed to overall experimental design and analysis. C. Ma and N. Zhang wrote the manuscript.

Disclosures: The authors declare no competing interests exist.

Submitted: 19 July 2021
Revised: 29 April 2022
Accepted: 20 July 2022

References

Beltra, J.C., S. Manne, M.S. Abdel-Hakeem, M. Kurachi, J.R. Giles, Z. Chen, V. Casella, S.F. Ngiow, O. Khan, Y.J. Huang, et al. 2020. Developmental relationships of four exhausted CD8(+) T cell subsets reveals underlying transcriptional and epigenetic landscape control mechanisms. *Immunity*. 52:825–841.e8. https://doi.org/10.1016/j.immuni.2020.04.014

Borges da Silva, H., C. Peng, H. Wang, K.M. Wanhainen, C. Ma, S. Lopez, A. Khoruts, N. Zhang, and S.C. Jameson. 2020. Sensing of ATP via the purinergic receptor P2RX7 promotes CD8$^+$ Trm cell generation by enhancing their sensitivity to the cytokine TGF-β. *Immunity*. 53: 158–171.e6. https://doi.org/10.1016/j.immuni.2020.06.010

Brummelman, J., E.M.C. Mazza, G. Alvisi, F.S. Colombo, A. Grilli, J. Mikulak, D. Mavilio, M. Alloisio, F. Ferrari, E. Lopci, et al. 2018. High-dimensional single cell analysis identifies stem-like cytotoxic CD8(+) T cells infiltrating human tumors. *J. Exp. Med.* 215:2520–2535. https://doi.org/10.1084/jem.20180684

Casey, K.A., K.A. Fraser, J.M. Schenkel, A. Moran, M.C. Abt, L.K. Beura, P.J. Lucas, D. Artis, E.J. Wherry, K. Hogquist, et al. 2012. Antigen-independent differentiation and maintenance of effector-like resident memory T cells in tissues. *J. Immuno.* 188:4866–4875. https://doi.org/10.4049/jimmunol.1200402

Chen, S., J. Fan, M. Zhang, L. Qin, D. Dominguez, A. Long, G. Wang, R. Ma, H. Li, Y. Zhang, et al. 2019. CD73 expression on effector T cells sustained by TGF-β facilitates tumor resistance to anti-4-1BB/CD137 therapy. *Nat. Commun.* 10:150. https://doi.org/10.1038/s41467-018-08123-8

Dimitrov, S., T. Lange, C. Gouttefangeas, A.T.R. Jensen, M. Szczepanski, J. Lehnnolz, S. Soekadar, H.G. Rammensee, J. Born, and L. Besedovsky. 2019. $G\alpha_s$-coupled receptor signaling and sleep regulate integrin activation of human antigen-specific T cells. *J. Exp. Med.* 216:517–526. https://doi.org/10.1084/jem.20181169

Gabriel, S.S., C. Tsui, D. Chisanga, F. Weber, M. Llano-Leon, P.M. Gubser, L. Bartholin, F. Souza-Fonseca-Guimaraes, N.D. Huntington, W. Shi, et al. 2021. Transforming growth factor-b-regulated mTOR activity preserves cellular metabolism to maintain long-term T cell responses in chronic infection. *Immunity*. 54:1–17. https://doi.org/10.1016/j.immuni.2021.06.007

Giordano, M., C. Henin, J. Maurizio, C. Imbratta, P. Bourdely, M. Buferne, L. Baitsch, L. Vanhille, M.H. Sieweke, D.E. Speiser, et al. 2015. Molecular profiling of CD8 T cells in autochthonous melanoma identifies Maf as driver of exhaustion. *EMBO J.* 34:2042–2058. https://doi.org/10.15252/embj.201490786

Gupta, P.K., J. Godec, D. Wolski, E. Adland, K. Yates, K.E. Pauken, C. Cosgrove, C. Ledderose, W.G. Junger, S.C. Robson, et al. 2015. CD39 expression

identifies terminally exhausted CD8+ T cells. *PLoS Pathog.* 11:e1005177. https://doi.org/10.1371/journal.ppat.1005177

Hashimoto, M., A.O. Kamphorst, S.J. Im, H.T. Kissick, R.N. Pillai, S.S. Ramalingam, K. Araki, and R. Ahmed. 2018. CD8 T cell exhaustion in chronic infection and cancer: Opportunities for interventions. *Annu. Rev. Med.* 69:301–318. https://doi.org/10.1146/annurev-med-012017-043208

He, R., S. Hou, C. Liu, A. Zhang, Q. Bai, M. Han, Y. Yang, G. Wei, T. Shen, X. Yang, et al. 2016. Follicular CXCR5- expressing CD8(+) T cells curtail chronic viral infection. *Nature.* 537:412–428. https://doi.org/10.1038/nature19317

Hu, Y., W.H. Hudson, H. Kissick, A. Wieland, C.B. Medina, A.P. Baptista, C. Ma, W. Liao, R.N. Germain, S.J. Turley, et al. 2022. TGF-β regulates the stem-like state of PD-1+ TCF-1+ virus-specific CD8 T cells during chronic infection. *J. Exp. Med.* 219. https://doi.org/10.1084/jem.20211574

Hudson, W.H., J. Gensheimer, M. Hashimoto, A. Wieland, R.M. Valanparambil, P. Li, J.X. Lin, B.T. Konieczny, S.J. Im, G.J. Freeman, et al. 2019. Proliferating transitory T cells with an effector-like transcriptional signature emerge from PD-1(+) stem-like CD8(+) T cells during chronic infection. *Immunity.* 51:1043–1058.e4. https://doi.org/10.1016/j.immuni.2019.11.002

Hynes, R.O., and A. Naba. 2012. Overview of the matrisome--an inventory of extracellular matrix constituents and functions. *Cold Spring Harb. Perspect. Biol.* 4:a004903. https://doi.org/10.1101/cshperspect.a004903

Im, S.J., M. Hashimoto, M.Y. Gerner, J. Lee, H.T. Kissick, M.C. Burger, Q. Shan, J.S. Hale, J. Lee, T.H. Nasti, et al. 2016. Defining CD8+ T cells that provide the proliferative burst after PD-1 therapy. *Nature.* 537:417–421. https://doi.org/10.1038/nature19330

Im, S.J., B.T. Konieczny, W.H. Hudson, D. Masopust, and R. Ahmed. 2020. PD-1+ stemlike CD8 T cells are resident in lymphoid tissues during persistent LCMV infection. *Proc. Natl. Acad. Sci. USA.* 117:4292–4299. https://doi.org/10.1073/pnas.1917298117

Jansen, C.S., N. Prokhnevska, V.A. Master, M.G. Sanda, J.W. Carlisle, M.A. Bilen, M. Cardenas, S. Wilkinson, R. Lake, A.G. Sowalsky, et al. 2019. An intra-tumoral niche maintains and differentiates stem-like CD8 T cells. *Nature.* 576:465–470. https://doi.org/10.1038/s41586-019-1836-5

Kurtulus, S., A. Madi, G. Escobar, M. Klapholz, J. Nyman, E. Christian, M. Pawlak, D. Dionne, J. Xia, O. Rozenblatt-Rosen, et al. 2019. Checkpoint blockade immunotherapy induces dynamic changes in PD-1(-)CD8(+) tumor-infiltrating T cells. *Immunity.* 50:181–194.e6. https://doi.org/10.1016/j.immuni.2018.11.014

Leong, Y.A., Y. Chen, H.S. Ong, D. Wu, K. Man, C. Deleage, M. Minnich, B.J. Meckiff, Y. Wei, Z. Hou, et al. 2016. CXCR5(+) follicular cytotoxic T cells control viral infection in B cell follicles. *Nat. Immunol.* 17:1187–1196. https://doi.org/10.1038/ni.3543

Li, S., M. Liu, M.H. Do, C. Chou, E.G. Stamatiades, B.G. Nixon, W. Shi, X. Zhang, P. Li, S. Gao, et al. 2020. Cancer immunotherapy via targeted TGF-β signalling blockade in TH cells. *Nature.* 587:121–125. https://doi.org/10.1038/s41586-020-2850-3

Liao, W., Y. Liu, C. Ma, L. Wang, G. Li, S. Mishra, S. Srinivasan, K.K.H. Fan, H. Wu, Q. Li, et al. 2021. The downregulation of IL-18R defines bona fide kidney-resident CD8(+) T cells. *iScience.* 24:101975. https://doi.org/10.1016/j.isci.2020.101975

Liu, M., F. Kuo, K.J. Capistrano, D. Kang, B.G. Nixon, W. Shi, C. Chou, M.H. Do, E.G. Stamatiades, S. Gao, et al. 2020. TGF-β suppresses type 2 immunity to cancer. *Nature.* 587:115–120. https://doi.org/10.1038/s41586-020-2836-1

Ma, C., S. Mishra, E.L. Demel, Y. Liu, and N. Zhang. 2017. TGF-β controls the formation of kidney-resident T cells via promoting effector T cell extravasation. *J. Immunol.* 198:749–756. https://doi.org/10.4049/jimmunol.1601500

Ma, C., and N. Zhang. 2015. Transforming growth factor-β signaling is constantly shaping memory T-cell population. *Proc. Natl. Acad. Sci. USA.* 112:11013–11017. https://doi.org/10.1073/pnas.1510119112

Mackay, L.K., A. Rahimpour, J.Z. Ma, N. Collins, A.T. Stock, M.L. Hafon, J. Vega-Ramos, P. Lauzurica, S.N. Mueller, T. Stefanovic, et al. 2013. The developmental pathway for CD103(+)CD8+ tissue-resident memory T cells of skin. *Nat. Immunol.* 14:1294–1301. https://doi.org/10.1038/ni.2744

Mariathasan, S., S.J. Turley, D. Nickles, A. Castiglioni, K. Yuen, Y. Wang, E.E. Kadel III, H. Koeppen, J.L. Astarita, R. Cubas, et al. 2018. TGFβ attenuates tumour response to PD-L1 blockade by contributing to exclusion of T cells. *Nature.* 554:544–548. https://doi.org/10.1038/nature25501

McLane, L.M., M.S. Abdel-Hakeem, and E.J. Wherry. 2019. CD8 T cell exhaustion during chronic viral infection and cancer. *Annu. Rev. Immunol.* 37:457–495. https://doi.org/10.1146/annurev-immunol-041015-055318

Miller, B.C., D.R. Sen, R. Al Abosy, K. Bi, Y.V. Virkud, M.W. LaFleur, K.B. Yates, A. Lako, K. Felt, G.S. Naik, et al. 2019. Subsets of exhausted CD8(+) T cells differentially mediate tumor control and respond to checkpoint blockade. *Nat. Immunol.* 20:326–336. https://doi.org/10.1038/s41590-019-0312-6

Milner, J.J., C. Toma, B. Yu, K. Zhang, K. Omilusik, A.T. Phan, D. Wang, A.J. Getzler, T. Nguyen, S. Crotty, et al. 2017. Runx3 programs CD8(+) T cell residency in non-lymphoid tissues and tumours. *Nature.* 552:253–257. https://doi.org/10.1038/nature24993

Miron, M., B.V. Kumar, W. Meng, T. Granot, D.J. Carpenter, T. Senda, D. Chen, A.M. Rosenfeld, B. Zhang, H. Lerner, et al. 2018. Human lymph nodes maintain TCF-1(hi) memory T cells with high functional potential and clonal diversity throughout life. *J. Immunol.* 201:2132–2140. https://doi.org/10.4049/jimmunol.1800716

Mylvaganam, G.H., D. Rios, H.M. Abdelaal, S. Iyer, G. Tharp, M. Mavigner, S. Hicks, A. Chahroudi, R. Ahmed, S.E. Bosinger, et al. 2017. Dynamics of SIV-specific CXCR5+ CD8 T cells during chronic SIV infection. *Proc. Natl. Acad. Sci. USA.* 114:1976–1981. https://doi.org/10.1073/pnas.1621418114

Park, B.V., Z.T. Freeman, A. Ghasemzadeh, M.A. Chattergoon, A. Rutebemberwa, J. Steigner, M.E. Winter, T.V. Huynh, S.M. Sebald, S.J. Lee, et al. 2016. TGFβ1-mediated SMAD3 enhances PD-1 expression on antigen-specific T cells in cancer. *Cancer Discov.* 6:1366–1381. https://doi.org/10.1158/2159-8290.CD-15-1347

Sade-Feldman, M., K. Yizhak, S.L. Bjorgaard, J.P. Ray, C.G. de Boer, R.W. Jenkins, D.J. Lieb, J.H. Chen, D.T. Frederick, M. Barzily-Rokni, et al. 2018. Defining T cell states associated with response to checkpoint immunotherapy in melanoma. *Cell.* 175:998–1013.e20. https://doi.org/10.1016/j.cell.2018.10.038

Sheridan, B.S., Q.M. Pham, Y.T. Lee, L.S. Cauley, L. Puddington, and L. Lefrancois. 2014. Oral infection drives a distinct population of intestinal resident memory CD8(+) T cells with enhanced protective function. *Immunity.* 40:747–757. https://doi.org/10.1016/j.immuni.2014.03.007

Siddiqui, I., K. Schaeuble, V. Chennupati, S.A. Fuertes Marraco, S. Calderon-Copete, D. Pais Ferreira, S.J. Carmona, L. Scarpellino, D. Gfeller, S. Pradervand, et al. 2019. Intratumoral Tcf1(+)PD-1(+)CD8(+) T cells with stem-like properties promote tumor control in response to vaccination and checkpoint blockade immunotherapy. *Immunity.* 50:195–211.e10. https://doi.org/10.1016/j.immuni.2018.12.021

Takimoto, T., Y. Wakabayashi, T. Sekiya, N. Inoue, R. Morita, K. Ichiyama, R. Takahashi, M. Asakawa, G. Muto, T. Mori, et al. 2010. Smad2 and Smad3 are redundantly essential for the TGF-β-mediated regulation of regulatory T plasticity and Th1 development. *J. Immunol.* 185:842–855. https://doi.org/10.4049/jimmunol.0904100

Tauriello, D.V.F., S. Palomo-Ponce, D. Stork, A. Berenguer-Llergo, J. Badia-Ramentol, M. Iglesias, M. Sevillano, S. Ibiza, A. Canellas, X. Hernando-Momblona, et al. 2018. TGFβ drives immune evasion in genetically reconstituted colon cancer metastasis. *Nature.* 554:538–543. https://doi.org/10.1038/nature25492

Tinoco, R., V. Alcalde, Y. Yang, K. Sauer, and E.I. Zuniga. 2009. Cell-intrinsic transforming growth factor-β signaling mediates virus-specific CD8+ T cell deletion and viral persistence in vivo. *Immunity.* 31:145–157. https://doi.org/10.1016/j.immuni.2009.06.015

Utzschneider, D.T., M. Charmoy, V. Chennupati, L. Pousse, D.P. Ferreira, S. Calderon-Copete, M. Danilo, F. Alfei, M. Hofmann, D. Wieland, et al. 2016. T cell factor 1-expressing memory-like CD8(+) T cells sustain the immune response to chronic viral infections. *Immunity.* 45:415–427. https://doi.org/10.1016/j.immuni.2016.07.021

Wu, J., A. Madi, A. Mieg, A. Hotz-Wagenblatt, N. Weisshaar, S. Ma, K. Mohr, T. Schlimbach, M. Hering, H. Borgers, and G. Cui. 2020. T cell factor 1 suppresses CD103+ lung tissue-resident memory T cell development. *Cell Rep.* 31:107484. https://doi.org/10.1016/j.celrep.2020.03.048

Wu, T., Y. Ji, E.A. Moseman, H.C. Xu, M. Manglani, M. Kirby, S.M. Anderson, R. Handon, E. Kenyon, A. Elkahloun, et al. 2016. The TCF1-Bcl6 axis counteracts type I interferon to repress exhaustion and maintain T cell stemness. *Sci. Immunol.* 1:eaai8593. https://doi.org/10.1126/sciimmunol.aai8593

Zander, R., D. Schauder, G. Xin, C. Nguyen, X. Wu, A. Zajac, and W. Cui. 2019. CD4(+) T cell help is required for the formation of a cytolytic CD8(+) T cell subset that protects against chronic infection and cancer. *Immunity.* 51:1028–1042.e4. https://doi.org/10.1016/j.immuni.2019.10.009

Zhang, N., and M.J. Bevan. 2012. TGF-β signaling to T cells inhibits autoimmunity during lymphopenia-driven proliferation. *Nat. Immunol.* 13:667–673. https://doi.org/10.1038/ni.2319

Zhang, N., and M.J. Bevan. 2013. Transforming growth factor-β signaling controls the formation and maintenance of gut-resident memory T cells by regulating migration and retention. *Immunity.* 39:687–696. https://doi.org/10.1016/j.immuni.2013.08.019

JEM

Supplemental material

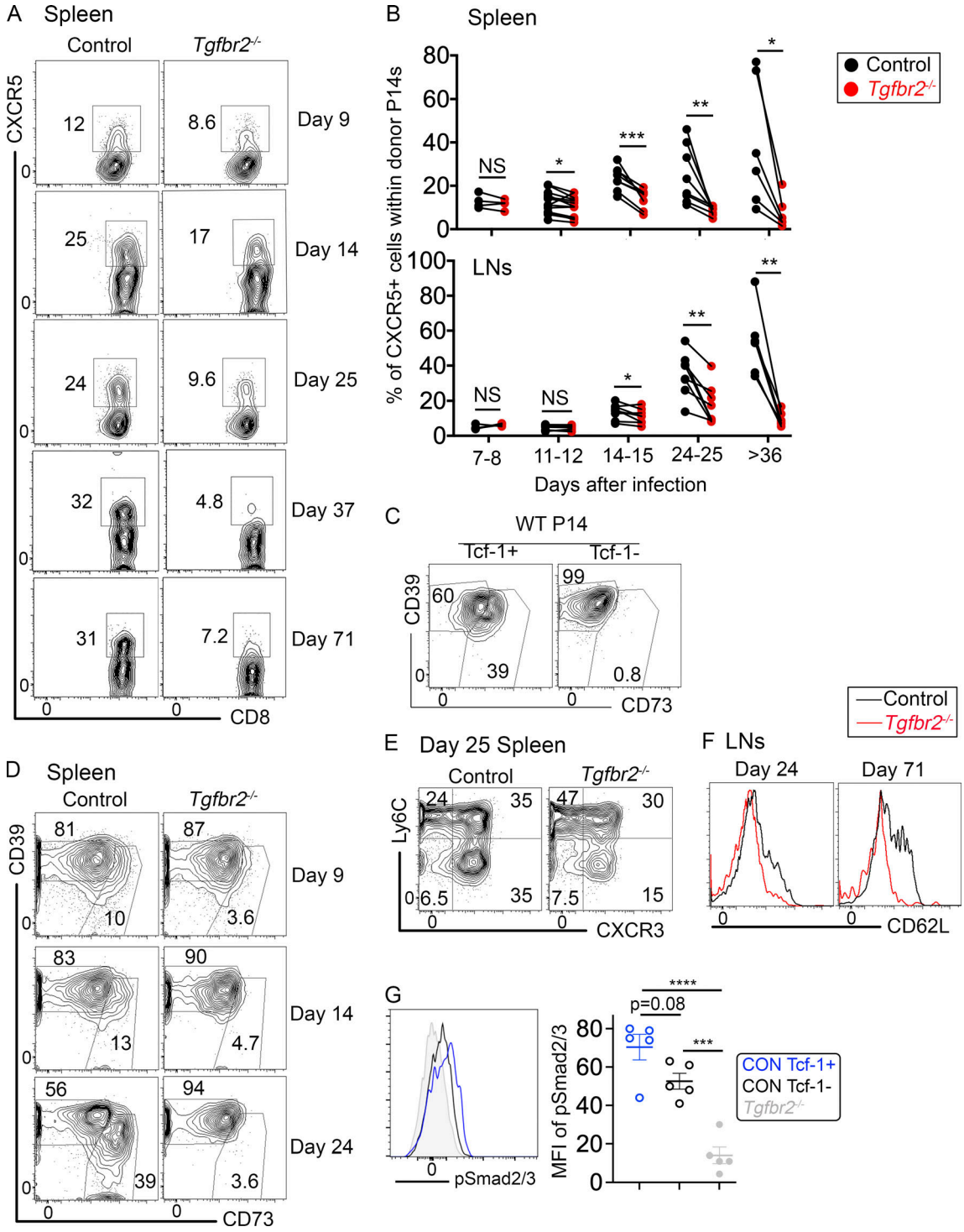

Figure S1. **Defective stem-like CD8⁺ T cell maintenance in the absence of TGF-β signaling.** Same experimental setup as in Fig. 1. **(A)** At indicated days after infection, the expression of CXCR5 on splenic P14 T cells was determined. **(B)** The percentage of CXCR5⁺ cells in donor P14 T cells is shown. Upper, spleen; lower, lymph nodes (LNs). Representative (A) or pooled (B) results from four independent experiments are shown (n = 4–14/time point). **(C)** Day 15–25 after infection, pre-gated Tcf-1⁺ and Tcf-1⁻ WT splenic P14 T cells were examined by flow cytometry. Representative FACS profiles from three independent experiments (n = 5/each) are shown. **(D–F)** Representative FACS profiles of pre-gated donor WT and *Tgfbr2*$^{-/-}$ P14 T cells are shown (three repeats, n = 10). Representative results from three independent experiments are shown. **(G)** Phosphorylated Smad2/3 was measured by FACS. Each symbol represents the results from an individual mouse. Pooled results from two independent experiments are shown in G (n = 5). *, P < 0.05; **, P < 0.01; ***, P < 0.001; and ****, P < 0.0001 by paired Student's t test (B) or one-way ANOVA (G).

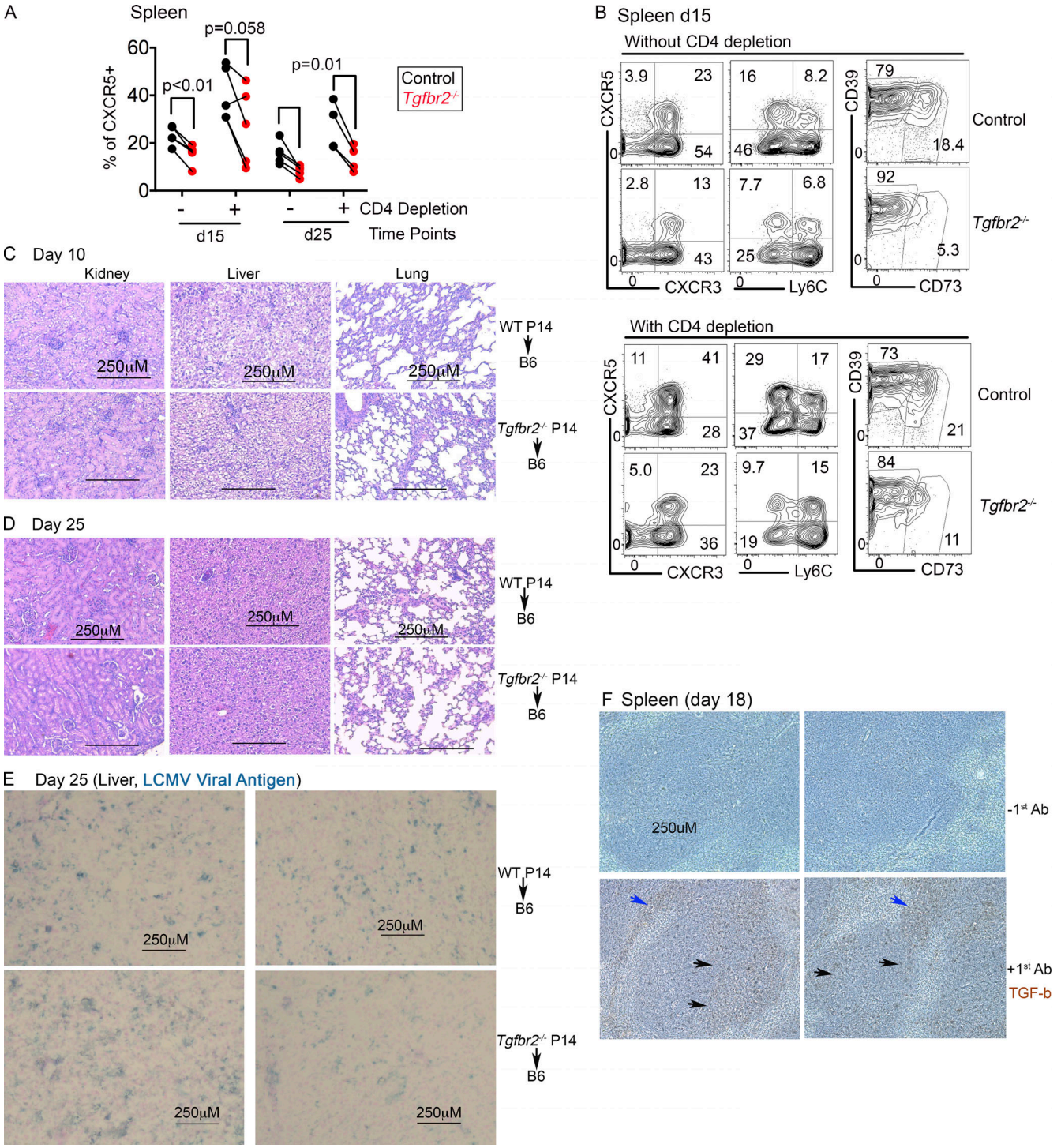

Figure S2. **Defective maintenance of CXCR5⁺ stem-like CD8⁺ T cells in the absence of TGF-β without apparent defects in viral clearance or pathology.** Similar experimental setup to Fig. 1. One group of mice received CD4 depleting antibody 1 d before and 1 d after infection. **(A)** The percentage of CXCR5⁺ cells in donor P14 T cells are shown at indicated time points. **(B)** Day 15 after infection, representative FACS profiles of pre-gated donor P14 T cells are shown (two independent repeats, *n* = 5/each). Each pair of symbols in A represents the results from an individual recipient. Pooled results from two independent repeats are shown in A (*n* = 5/each). P values were calculated by paired Student's *t* test. WT and *Tgfbr2*$^{-/-}$ P14 T cells were separately transferred into B6 recipients followed by LCMV Cl13 infection. **(C and D)** Day 10 (C) or day 25 (D) after infection, representative H&E staining of different tissues are shown (*n* = 3/each, two repeats). **(E)** Day 25 after infection, immunohistochemistry of liver sections to show LCMV antigen (blue). *n* = 3/each, two repeats. **(F)** Day 18 after LCMV Cl13 infection, spleen sections were examined by immunohistochemistry. Top, negative staining control without primary antibody; bottom, staining with primary antibody (two independent repeats, *n* = 2/each). Black arrows indicate intra-follicle TGF-β producing foci, and blue ones indicate extra-follicle TGF-β producing foci.

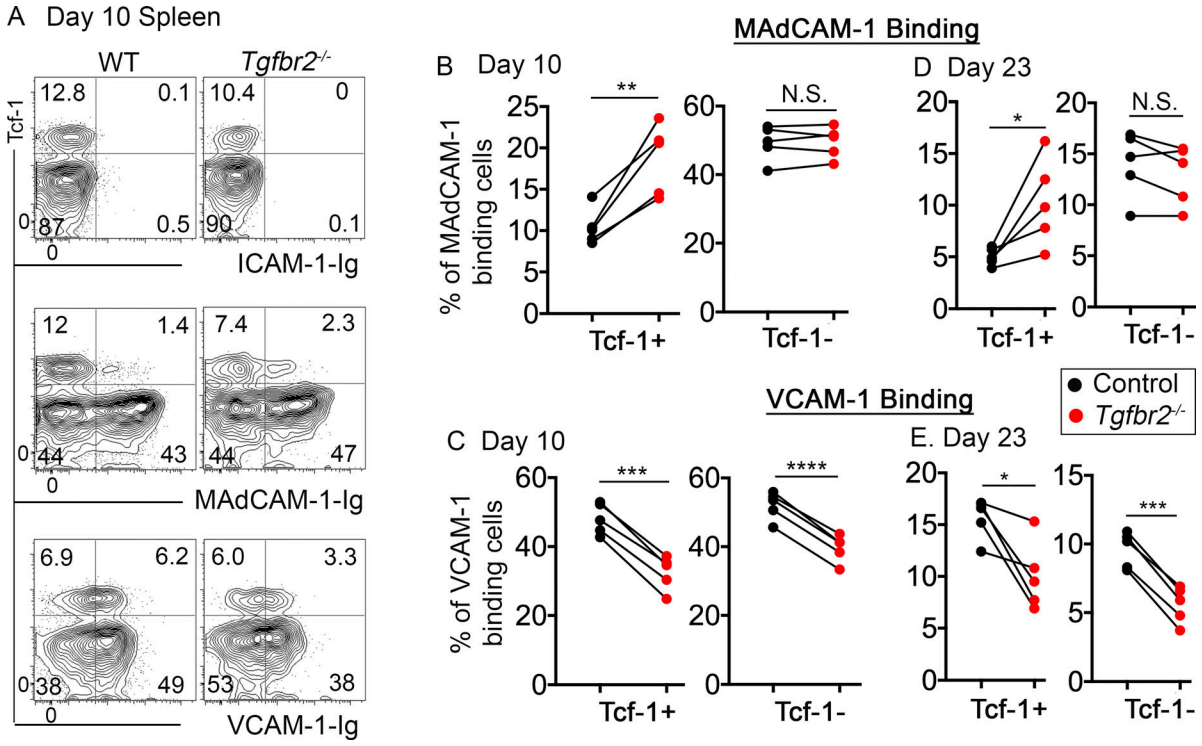

Figure S3. **Enhanced MAdCAM-1 and reduced VCAM-1 binding in the absence of TGF-β signaling**. ICAM-1 (intercellular adhesion molecule-1) mainly binds to β2-containing integrins and serves as a negative control. MAdCAM-1 binds to α4β7 while VCAM-1 binds to α4β1. Same experimental setup as in Fig. 1. Splenic P14 T cells were incubated with either ICAM-1-Ig, MAdCAM-1-Ig, or VCAM-1-Ig in the presence of GP_{33-41} at 37°C for 5 min followed by standard flow cytometry staining and analysis. **(A)** Representative FACS profiles of pre-gated WT control and *Tgfbr2*$^{-/-}$ P14 T cells are shown (three repeats, *n* = 5/each). **(B–E)** The percentage of MAdCAM-1 binding (B and D) or VCAM-1 binding (C and E) at day 10 (B and C) and day 23 (D and E) in pre-gated Tcf-1^{+} and Tcf-1^{-} P14 T cells are shown. Each pair of symbols in B–E represents the results from an individual recipient (three repeats, *n* = 5/each). *, P < 0.05; **, P < 0.01; ***, P < 0.001; and ****, P < 0.0001 by paired Student's *t* test.

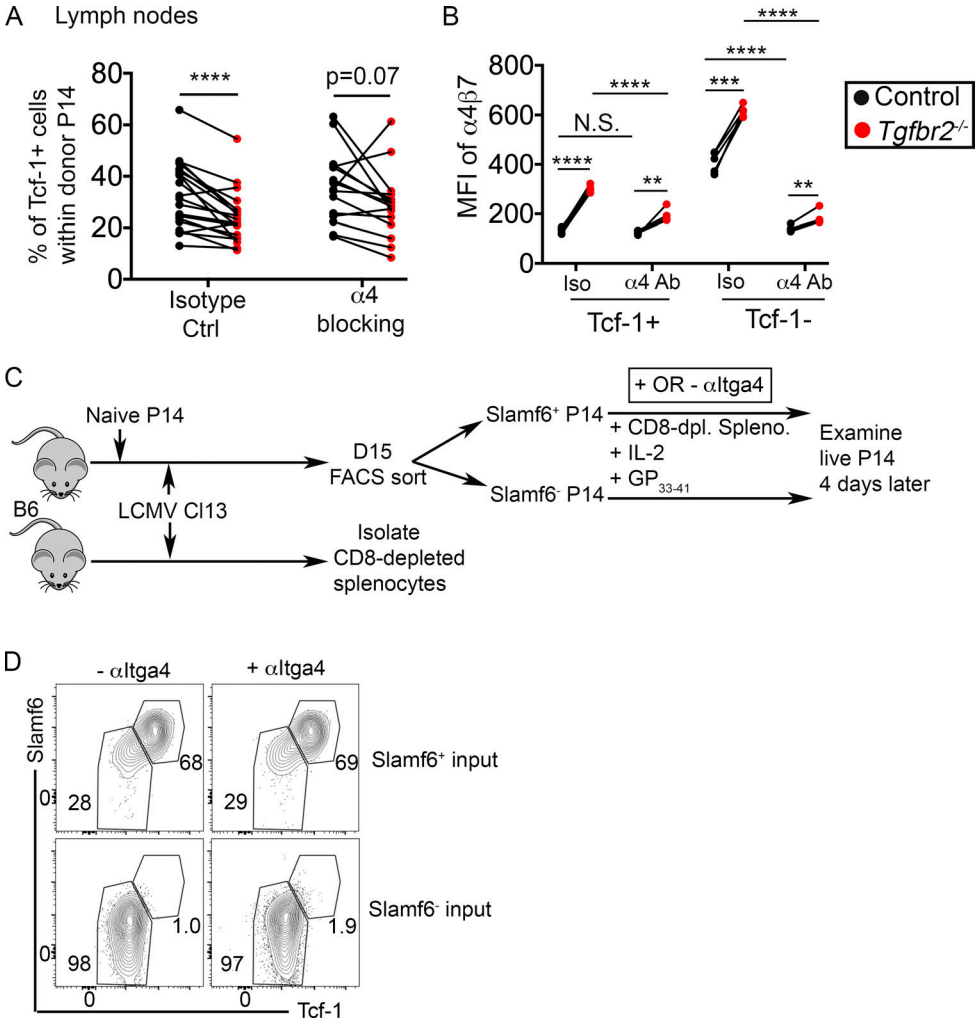

Figure S4. **Integrin α4 blocking rescues the defective maintenance of Tcf-1⁺ *Tgfbr2*$^{-/-}$ in vivo without directly interfering with Tcf-1⁺ cell differentiation in vitro.** Same experimental setup as in Fig. 5. **(A)** The percentage of Tcf-1⁺ cells in donor P14 T cells isolated from the lymph nodes are shown. **(B)** MFI of α4β7 on Tcf-1⁺ and Tcf-1⁻ donor P14s are shown. Each pair of symbols represents the results from an individual recipient. Pooled results from five independent experiments are shown in A (n = 15–20). Representative results from two independent experiments are shown in B (n = 5). **(C)** Experimental design for in vitro integrin α4 blocking. **(D)** Representative FACS profiles of pre-gated live P14 T cells after 4-d culture are shown. Representative results from two independent experiments (P14 T cells were pooled from five mice/each experiment as sorting input cells) are shown in D. **, P < 0.01; ***, P < 0.001; and ****, P < 0.0001 calculated by paired Student's t test.

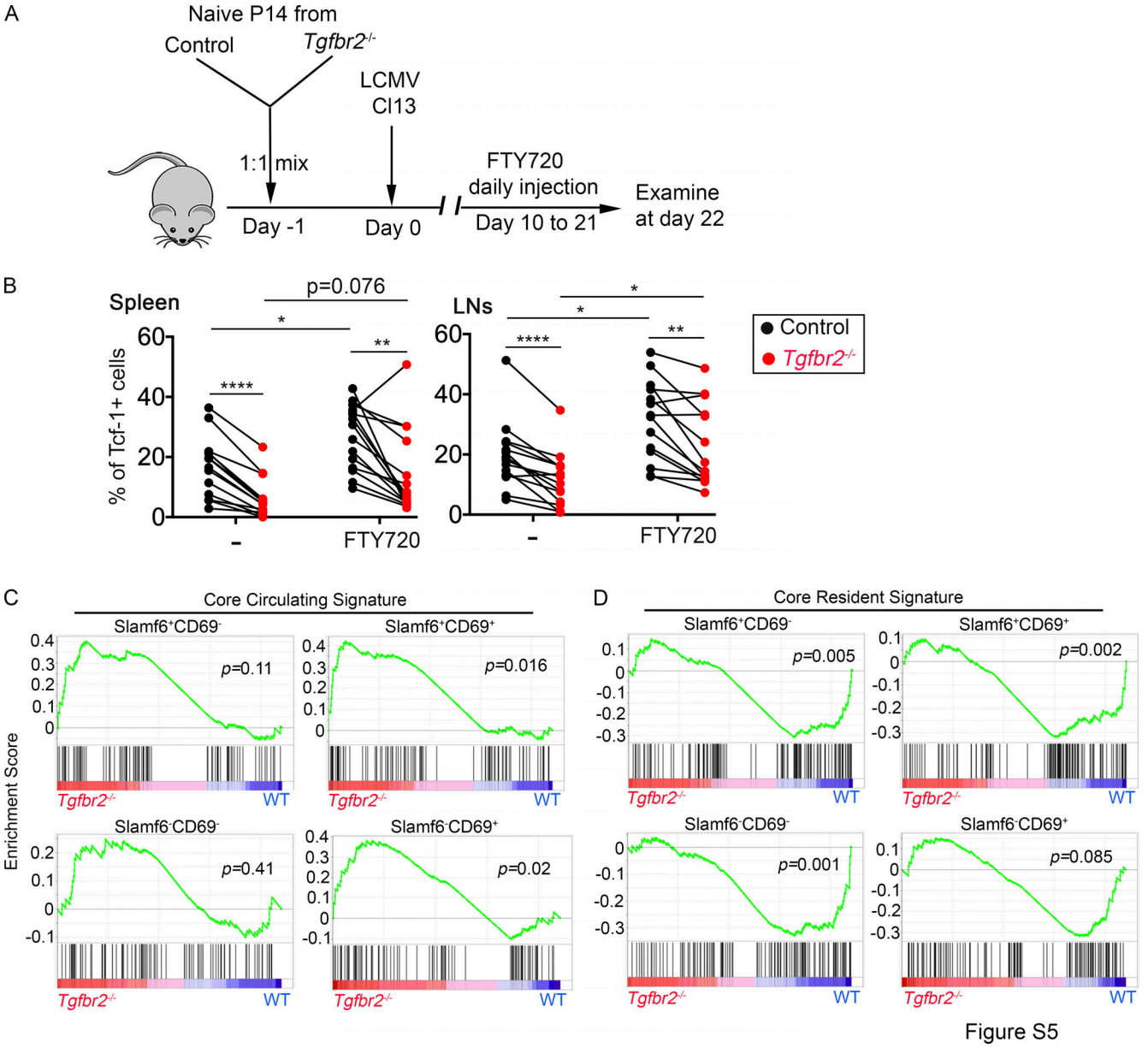

Figure S5. **TGF-β–dependent resident program in exhausted CD8⁺ T cells during chronic viral infection. (A)** Experimental setup for B. Briefly, naive P14 isolated from WT and *Tgfbr2*$^{-/-}$ mice were co-transferred into B6 recipients followed by LCMV Cl13 infection. Daily injection of FTY720 was started 10 d later. **(B)** The percentage of Tcf-1⁺ cells was determined on day 22 after infection by flow cytometry. Each pair of symbols in B represents the results from an individual recipient. Pooled results from three independent experiments are shown (n = 15). *, P < 0.05; **, P < 0.01; and ****, P < 0.0001 by Student's t test. **(C and D)** Similar experimental setup as in Fig. 1 A. Day 15 after infection, different subsets of control and *Tgfbr2*$^{-/-}$ P14 T cells were FACS sorted from pooled spleen and lymph nodes and subjected to bulk RNA-seq analysis. Gene set enrich analysis for core circulating memory T cells gene signature (C) and core resident memory T cell gene signature (D) are shown. For C and D, each group contain biological independent duplicates.